

January 2017

On thermal corrections to near-threshold annihilation

Seyong Kim^a and M. Laine^b^a*Department of Physics, Sejong University, Gunja-Dong 98, Seoul 143-747, South Korea*^b*AEC, Institute for Theoretical Physics, University of Bern,
Sidlerstrasse 5, CH-3012 Bern, Switzerland*

Abstract

We consider non-relativistic “dark” particles interacting through gauge boson exchange. At finite temperature, gauge exchange is modified in many ways: virtual corrections lead to Debye screening; real corrections amount to frequent scatterings of the heavy particles on light plasma constituents; mixing angles change. In a certain temperature and energy range, these effects are of order unity. Taking them into account in a resummed form, we estimate the near-threshold spectrum of kinetically equilibrated annihilating TeV scale particles. Weakly bound states are shown to “melt” below freeze-out, whereas with attractive strong interactions, relevant e.g. for gluinos, bound states boost the annihilation rate by a factor 4...80 with respect to the Sommerfeld estimate, thereby perhaps helping to avoid overclosure of the universe. Modestly non-degenerate dark sector masses and a way to combine the contributions of channels with different gauge and spin structures are also discussed.

1. Introduction

The possibility that stable or long-lived massive neutral particles could be responsible for dark matter, continues to motivate a versatile program of direct and indirect searches and collider experiments. The cosmological abundance of such particles is determined by a “freeze-out” process, taking place when the annihilation rate decreases below the Hubble rate. For particles of mass M , the freeze-out temperature is generically of order $T \sim M/25 \dots M/20$.¹ In this regime the particles are kinetically equilibrated and non-relativistic. Therefore they move slowly and have time to experience repeated interactions (cf. e.g. refs. [1–5]).

It is conceivable that repeated soft interactions could modify the nature of the annihilation process. For instance, it has been appreciated in recent years that in certain models there are attractive interactions between dark matter particles, or between particles co-annihilating with dark matter particles, which could lead to bound-state formation even in weakly interacting cases (cf. e.g. refs. [6–9]). A number of studies (cf. e.g. refs. [10–16]) have included bound states in a freeze-out analysis, notably by adding an on-shell bound state phase space distribution as an independent degree of freedom in a set of Boltzmann equations. A thereby increased annihilation rate might represent a phenomenologically welcome development, given that LHC searches have pushed up the dark matter mass scale, which could lead to the weakly interacting dark matter energy density overclosing the universe.

Treating bound states precisely is a non-trivial task, and furthermore quite sensitive to thermal effects [17]. In ref. [18], basic formulae for the inclusion of bound states on the perturbative and non-perturbative levels were derived, working within the framework of non-relativistic effective field theories [19, 20]. The formalism was also applied to a particular model, QCD at $T \gtrsim 150$ MeV. Both a perturbative and a lattice study found an enhancement of the singlet channel annihilation rate of bottom quarks by up to two orders of magnitude with respect to a previous estimate [21], which was based on a thermally averaged “Sommerfeld factor” [22–25], correcting the annihilation rate of free scatterers.

The purpose of the present paper is to apply the perturbative side of the approach of ref. [18] to simple examples in cosmology. In particular, we show that thermal corrections to the near-threshold spectrum (or the differential annihilation rate) are of order unity in a temperature range (eq. (2.3)) which may coincide with that of the freeze-out process. The effect on the total annihilation rate is in general small in weakly coupled systems, whereas in strongly coupled systems near-threshold annihilation can dominate the total rate.

To put the physics in a wider context, we note in passing that thermal corrections to annihilation phenomena have been addressed in great detail in the context of nuclear reactions in astrophysical plasmas (cf. ref. [26] for a review). Those processes resemble the present ones in the sense that the energy released is large compared with thermal scales, and that

¹This follows from $H \sim n\langle\sigma v\rangle$, i.e. $\frac{T^2}{m_{\text{Pl}}} \sim \left(\frac{MT}{2\pi}\right)^{3/2} e^{-M/T} \frac{\alpha^2}{M^2}$, where α is some fine-structure constant.

the annihilation process is accurately captured by effective four-particle operators. Of course, there is the qualitative difference that the Coulomb interaction between the non-relativistic ionized nuclei is repulsive, so that no bound states can form.

The paper is organized as follows. We start by discussing the energy and temperature scales relevant for non-relativistic annihilation in sec. 2. A thermally averaged s -wave annihilation rate and a corresponding spectral function are defined in sec. 3, where we also recall how these can be computed in resummed perturbation theory, accounting for collective plasma phenomena which yield the dominant thermal corrections. Sec. 4 contains an application of the formalism to the case of dark particles bound together by Standard Model Z exchange, sec. 5 to light dark Z' exchange, and sec. 6 to gluon exchange. In sec. 7 we discuss how the situation changes if the dark particles are modestly non-degenerate in mass, and in sec. 8 how different annihilation channels can be combined. Conclusions and an outlook are offered in sec. 9. In two appendices the transverse parts of thermal Z and Z' self-energies are computed at 1-loop order in a general R_ξ gauge, demonstrating the gauge independence of the structures that affect our thermal considerations.

2. Physics background: scales in a thermal medium

In order to introduce the various phenomena that play a role, we start by defining a number of energy and momentum scales affecting the dynamics. Subsequently examples of how the scales interfere with each other are outlined.

Non-relativistic energy and momentum. Kinetically equilibrated non-relativistic particles of mass M at a temperature T move with an average velocity $v \sim (T/M)^{1/2} \ll 1$ and have a kinetic energy $E_{\text{kin}} \sim Mv^2 \sim T \ll M$. If the particles interact through Coulomb-like exchange, the associated potential energy is $E_{\text{pot}} \sim \alpha/r \sim Mv\alpha$, where we expressed the typical distance between the annihilating particles, r , through the uncertainty relation as the inverse relative momentum, $r \sim 1/(Mv)$. For $v > \alpha$ the potential energy is small compared with the kinetic energy, but for $v \sim \alpha$ the two are of the same order, leading to Sommerfeld corrections of order unity. If the particles happen to form a bound state, they can no longer move freely, but we can still speak of an average velocity associated with the bound motion. In this case $E_{\text{kin}} \sim E_{\text{pot}}$ by definition, so that $v \sim \alpha$. Thereby the binding energy associated with bound states is $\Delta E \sim M\alpha^2$.

Thermal widths. An interacting particle gets constantly kicked by scatterings with plasma constituents. The scatterings imply that the particle has a finite “width”, or interaction rate. This does not mean that the particle would decay, but that it can change its phase or colour or momentum or go into an excited state. Parametrically, for a single heavy particle, the

width is $\Gamma_{\text{int}} \sim \alpha T$ [27]. (No momentum transfer is involved in these scatterings; if we wish to adjust momenta, the relevant concept is the kinetic equilibration rate, which scales as $\Gamma_{\text{kin}} \sim \alpha^2 T^2/M$ [28].) If we consider a pair of heavy particles attracting each other through gauge exchange, then the interaction rate is smaller than $2\Gamma_{\text{int}}$, because close to each other the particles would form a gauge singlet, which does not feel gauge interactions. In fact the width has a “dipole” shape at small separations, $\Gamma \sim \alpha^2 T^3 r^2$ [29]. Inserting $r \sim 1/(Mv)$, this leads to $\Gamma \sim \alpha^2 T^2/M$ for scattering states, and $\Gamma \sim T^3/M^2$ for bound states. In the case of scattering states, with $E \sim T$, the width plays a subleading role, whereas for bound states the issue is more subtle and is discussed below.

Thermal masses. Apart from thermal widths, thermal effects also lead to “virtual corrections”, notably thermal masses. For electric fields responsible for the Coulomb-like exchange, the thermal mass is known as a Debye mass and is of order $m_{\text{th}} \sim \alpha^{1/2} T$. This defines the distance scale at which gauge exchange varies; for instance, the width defined above is of the form $\Gamma \sim \Gamma_{\text{int}} \Phi(m_{\text{th}} r)$, with $\Phi(x) \sim x^2$ for $x \ll 1$ and $\Phi(x) = 2$ for $x \gg 1$.

The heavy particles also experience thermal mass shifts. An unresummed perturbative computation yields $\delta M_{\text{th}} \sim \alpha T^2/M$ [30],² however the Debye screening of the electric field leads to a correction with a different structure and an opposite sign (cf. eq. (7.15)),

$$\delta M_{\text{rest,th}} = -\frac{1}{2} \alpha m_{\text{th}} \sim -\alpha^{3/2} T. \quad (2.1)$$

If $T < \alpha^{1/2} M$, as is the case in our considerations, the latter correction dominates. This is the case in general: unresummed perturbation theory leads to power-suppressed thermal corrections, but collective plasma phenomena yield larger effects (a nice discussion can be found in sec. 6 of ref. [32]). In the context of nuclear rates eq. (2.1) amounts to a “Salpeter correction” (cf. ref. [26] for a review), which increases the annihilation rate by a factor $\exp(-2\delta M_{\text{rest,th}}/T) = \exp(\alpha m_{\text{th}}/T)$. This is a correction of $\mathcal{O}(\alpha^{3/2})$ to the total rate, but an $\mathcal{O}(1)$ effect close to the threshold, given that its location gets shifted.

When does the Sommerfeld effect play a role for annihilation? Consider scattering states with $v \sim (T/M)^{1/2}$. As discussed above, the potential energy from a Coulomb exchange is of the same order as the kinetic energy for $v \sim \alpha$. Therefore, from $(T/M)^{1/2} \sim \alpha$, we find that the Sommerfeld effect is of order unity for

$$T \sim \alpha^2 M. \quad (2.2)$$

In contrast, in the range $T \gtrsim \alpha M$ to be defined in eq. (2.3), where $v \gtrsim \alpha^{1/2}$, E_{pot} only represents a subset of higher-order corrections. It may be noted that the momenta exchanged

²In the dark matter context mass corrections of this type were considered and shown to be small in ref. [31].

by scattering states are large compared with Debye masses, $Mv \sim (MT)^{1/2} \gg m_{\text{th}} \sim \alpha^{1/2}T$, and the kinetic energy of the annihilating pair is large compared with its thermal width, $T \gg \Gamma \sim \alpha^2 T^2/M$. Therefore thermal effects can be omitted from Sommerfeld considerations at leading order in α [21]. However we do expect an effect of $\mathcal{O}(\alpha^{3/2})$ as shown by eq. (2.1), and return to a discussion of the magnitude of thermal effects below eq. (3.10).

When do bound states exist in a thermal medium? Consider an *attractive* Coulomb-like exchange, $V(r) = -\alpha/r$. A conservative estimate asserts that bound states “melt” when the thermal screening length (inverse of m_{th}) has become shorter than the Bohr radius [17], $1/(\alpha^{1/2}T) \lesssim 1/(\alpha M)$, i.e. $T \gtrsim \alpha^{1/2}M$. A more stringent estimate is obtained by requiring that the thermal width exceeds the binding energy: $\Gamma \sim T^3/M^2 \gtrsim \Delta E \sim \alpha^2 M$, i.e. $T \gtrsim \alpha^{2/3}M$ [33–35]. However it is difficult to fix the prefactor of this estimate, and therefore to decide whether in the case of weak interactions, with $\alpha \sim 10^{-2}$, bound states can persist up to the temperatures $T \sim M/25 \dots M/20$ that are relevant for the freeze-out analysis. A numerical investigation is carried out for various models in secs. 4 and 5, cf. figs. 3 and 4. For simple power counting, we consider the regime

$$T \gtrsim \alpha M \tag{2.3}$$

for this purpose, in which case bound states exist at $T \sim \alpha M$ and then melt at $T \gg \alpha M$, i.e. thermal corrections are of order unity. In practice the gauge exchange is typically Yukawa screened, but for simplicity we use the Coulombic estimate in the following.

When do bound states play a role for annihilation? If bound states exist, they have a binding energy $\Delta E \sim M\alpha^2$. The Boltzmann weight is then boosted by a factor $\exp(\Delta E/T)$, implying that bound states have an effect of order unity for $T \sim \alpha^2 M$, just like the Sommerfeld effect in eq. (2.2). In the regime of eq. (2.3), in contrast, bound-state contributions amount to higher-order corrections to the total annihilation rate, because $\Delta E/T \lesssim \alpha$. A strongly interacting case in which bound states do dominate the total annihilation rate is discussed in sec. 6, cf. fig. 5.

3. Theoretical framework

In order to address the phenomena outlined above, we formulate a specific theoretical framework. We start by defining a thermally averaged annihilation rate in the non-relativistic regime (sec. 3.1); show how the energy scales contributing to the thermal annihilations can be resolved through a spectral function (sec. 3.2); recall how the spectral function can be determined (beyond strict perturbation theory) through the solution of an inhomogeneous Schrödinger equation (sec. 3.3); and discuss how the “static potential” appearing in the

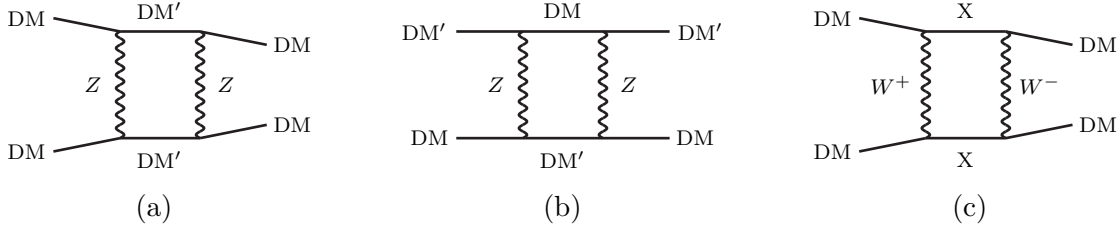


Figure 1: Examples of processes with static gauge exchange. Left: with neutral gauge exchange, the particle identity remains the same in the case of fermions ($DM' = DM$) but changes for scalars ($DM' \neq DM$). The diagram illustrates the kinematics for the case $m_{DM'} > m_{DM}$. Middle: another possibility for gauge exchange. A further one, relevant for certain models, can be obtained by exchanging DM and DM' in the intermediate stage. Right: with charged gauge exchange, particle identity necessarily changes ($X \neq DM$). If $m_X \gg m_{DM}$, only Z exchange needs to be considered.

Schrödinger equation can be computed within a thermal plasma (sec. 3.4). We refer to the heavy particles as DM and DM', even though the two species can also be the same (cf. fig. 1).

3.1. Thermally averaged annihilation rate and equilibrium number density

Let $\eta\theta$ stand for a local operator which annihilates a DM'-DM pair. Eigenstates of the Hamiltonian containing a DM'-DM pair, either a bound or a scattering state, are denoted by $|m\rangle$ and have energies $E_m \sim 2M$.³ Within non-relativistic theories [19], inclusive s -wave DM'-DM annihilations can be described by local four-particle operators of the type $\mathcal{O} = ic_1\alpha^2\theta^\dagger\eta^\dagger\eta\theta/M^2$ [20], where α is a fine structure constant evaluated at a hard renormalization scale $\sim 2M$ and c_1 is a group-theoretic coefficient. Within a thermal medium, the annihilations mediated by this operator define a “chemical equilibration rate”, Γ_{chem} , implying that the dark matter density n evolves as

$$(\partial_t + 3H)n = -\Gamma_{\text{chem}}(n - n_{\text{eq}}) + \mathcal{O}(n - n_{\text{eq}})^2. \quad (3.1)$$

Here H is the Hubble rate and n_{eq} is the DM equilibrium number density. Through a linear response analysis, Γ_{chem} can be related to an equilibrium 2-point correlator and then expressed as a “transport coefficient” [36]. Within the NRQCD framework the transport coefficient turns out to be proportional to the intuitively transparent thermal expectation value [18]

$$\gamma \equiv \frac{1}{\mathcal{Z}} \sum_m e^{-E_m/T} \langle m | \theta^\dagger \eta^\dagger \eta \theta | m \rangle, \quad (3.2)$$

³For simplicity of notation we assume the system to be placed in a large periodic box, so that the spectrum of scattering states is discrete, however in the end the thermodynamic limit is taken.

as $\Gamma_{\text{chem}} \approx 8c_1\alpha^2\gamma/(M^2n_{\text{eq}})$. Linearizing a dark matter Boltzmann equation [37, 38]⁴, *viz.*

$$(\partial_t + 3H)n \simeq -\langle\sigma v\rangle(n^2 - n_{\text{eq}}^2), \quad (3.3)$$

we can identify $\langle\sigma v\rangle = \Gamma_{\text{chem}}/(2n_{\text{eq}})$ and therefore get $\langle\sigma v\rangle \approx 4c_1\alpha^2\gamma/(M^2n_{\text{eq}}^2)$. If the DM and DM' particles have N internal degrees of freedom, then in the free limit $\gamma \rightarrow \gamma_{\text{free}} = n_{\text{eq}}^2/(4N)$, cf. the discussion below eq. (3.18). A further useful quantity, closely related to $\langle\sigma v\rangle$, is a “thermally averaged Sommerfeld factor”, characterizing the strength of interactions: $\bar{S}_1 \equiv \gamma/\gamma_{\text{free}} = 4N\gamma/n_{\text{eq}}^2$. Thereby $\langle\sigma v\rangle \approx c_1\alpha^2\bar{S}_1/(M^2N)$.

In order to solve eq. (3.1) or (3.3), we need to know the value of n_{eq} , and if we discuss radiative corrections to Γ_{chem} or $\langle\sigma v\rangle$, we should also discuss those to n_{eq} . In order to compute such corrections, n_{eq} has to be properly defined. As suggested in ref. [36], it is physically meaningful to define $n \equiv e/M$, where e is the energy density carried by the dark matter particles. However, if dark matter is made of “particles” and “antiparticles”, a simpler definition is provided by the susceptibility related to a conserved Noether charge: $n_{\text{eq}} \equiv \chi_f \equiv \frac{1}{V}\langle Q^2 \rangle$ where V is the volume and, for fermions, $Q = \int_{\mathbf{x}} \bar{\psi}\gamma_0\psi$. Indeed, evaluating this in the energy eigenbasis, we get $n_{\text{eq}} = \frac{2}{\mathcal{Z}V} \sum_{\mathbf{p}} e^{-\mathcal{E}_p/T} + \mathcal{O}(e^{-2M/T})$, where \mathcal{E}_p are the energy eigenvalues for states with a single heavy particle and the factor 2 accounts for the antiparticles. Going over to infinite volume and carrying out a resummed next-to-leading order (NLO) computation, we find

$$n_{\text{eq}} = 2N \int_{\mathbf{p}} e^{-\mathcal{E}_p/T} \left[1 - \frac{g^2 T^2 C_R}{12p^2} + \frac{g^2 m_{\text{th}} C_R}{8\pi T} + \mathcal{O}(g^4, e^{-M/T}) \right], \quad \mathcal{E}_p \equiv \sqrt{p^2 + M^2}, \quad (3.4)$$

where C_R is the quadratic Casimir of the gauge representation, M corresponds technically to a pole mass, and m_{th} is the Debye mass defined around eq. (2.1). Through partial integrations it can be shown that the first correction amounts to the thermal mass of refs. [30, 31], $M^2 \rightarrow M_{\text{th}}^2 \equiv M^2 + \Delta M_{\text{th}}^2$, with $\Delta M_{\text{th}}^2 = g^2 T^2 C_R/6$. Both the “rest” and “kinetic” masses get corrected by the same amount. The second correction amounts to the Salpeter term in eq. (2.1), which only affects the rest mass. The latter term dominates if $T \ll gM$, because the average momentum is $p^2 \simeq MT$. This formally dominant contribution was omitted in the unresummed computations of refs. [30, 31], and can only be found by properly incorporating Debye screening in the gauge field propagator. If we “resum” both corrections into the exponent and denote $\alpha \equiv g^2 C_R/(4\pi)$, then

$$n_{\text{eq}} \approx 2N \left(\frac{M_{\text{th}} T}{2\pi} \right)^{3/2} \exp\left(-\frac{M_{\text{th}}}{T} + \frac{\alpha m_{\text{th}}}{2T} \right). \quad (3.5)$$

We note that in γ/n_{eq}^2 , which appears in $\langle\sigma v\rangle$ and \bar{S}_1 defined below eq. (3.3), the latter term in the exponent cancels against the Salpeter correction discussed below eq. (2.1).

⁴For simplicity we consider a single DM species here (with DM' equivalent or antiparticle to DM), with N internal degrees of freedom; systems with multiple non-degenerate species are addressed in secs. 6 and 7.

3.2. Definition of a spectral function

We now wish to resolve the total rate in eq. (3.2) into a spectral representation, which tells which kind of states are responsible for the annihilations. For this purpose we first define a Wightman function,

$$\Pi_{<}(\omega) \equiv \int_{-\infty}^{\infty} dt e^{i\omega t} \langle (\theta^\dagger \eta^\dagger)(0, \mathbf{0}) (\eta \theta)(t, \mathbf{0}) \rangle_T, \quad (3.6)$$

where $\langle \dots \rangle_T$ refers to a thermal expectation value and ω corresponds to the energy released in the hard process. Clearly, the full rate in eq. (3.2) is obtained from the integral over all possibilities,

$$\gamma = \int_{-\infty}^{\infty} \frac{d\omega}{2\pi} \Pi_{<}(\omega). \quad (3.7)$$

Now, for a better physical understanding, we re-express eq. (3.7) in terms of a central underlying object, the *spectral function*. In operator language it is defined as

$$\rho(\omega, \mathbf{k}) \equiv \int_{-\infty}^{\infty} dt \int_{\mathbf{r}} e^{i(\omega t - \mathbf{k} \cdot \mathbf{r})} \left\langle \frac{1}{2} [(\eta \theta)(t, \mathbf{r}), (\theta^\dagger \eta^\dagger)(0, \mathbf{0})] \right\rangle_T. \quad (3.8)$$

We refer to $k \equiv |\mathbf{k}|$ as the total momentum of the pair with respect to the heat bath. All other 2-point correlators can be expressed in terms of the spectral function, in particular $\Pi_{<}(\omega) = 2n_B(\omega) \int_{\mathbf{k}} \rho(\omega, \mathbf{k})$, where n_B is the Bose distribution. Inserting this information into eq. (3.7), assuming $\pi T \ll M$, and noting that there is spectral weight only at $\omega \gtrsim 2M$, we obtain

$$\gamma = \int_{2M-\Lambda}^{\infty} \frac{d\omega}{\pi} e^{-\omega/T} \int_{\mathbf{k}} \rho(\omega, \mathbf{k}) + \mathcal{O}(e^{-4M/T}), \quad \alpha^2 M \ll \Lambda \lesssim M. \quad (3.9)$$

The cutoff Λ plays no practical role as long as it is $\gg \alpha^2 M$, given that the spectral function vanishes for $0 \ll \omega \ll 2M$,⁵ nevertheless we introduce it in order to restrict the average to a regime in which a non-relativistic treatment and the replacement of the Bose distribution through the Boltzmann distribution are formally justified.

We note that the spectral function is a nice object because it is of $\mathcal{O}(1)$ rather than exponentially suppressed; the exponential suppression has been factored into eq. (3.9). In the following we sometimes refer to ρ as a *differential annihilation rate*, with the understanding that ρ is to be weighted by $e^{-\omega/T}$ to properly fill this role.

A final ingredient for applying eq. (3.9) is to note that, as usual in a non-relativistic two-body problem, the dependence on the total momentum \mathbf{k} factorizes from the internal dynamics. Therefore it is sufficient to compute $\rho(\omega, \mathbf{k})$ for $\mathbf{k} = \mathbf{0}$, and recall afterwards that for $\mathbf{k} \neq \mathbf{0}$ the center-of-mass energy is $2M + k^2/(4M)$ rather than $2M$, cf. eq. (3.11).

⁵To be precise, at finite temperature the spectral function does not vanish exactly in this regime but has a small tail [39]; the corresponding contribution to γ is suppressed by α and powers of T/M .

3.3. Ways to determine the spectral function

According to eq. (3.9), we need to determine the spectral function in the range

$$|\omega - 2M| \lesssim \pi T \ll M. \quad (3.10)$$

This puts us deep in the non-relativistic regime. In principle, spectral functions can be computed in strict perturbation theory both in vacuum and including thermal corrections. Thermal corrections can be shown to be infrared (IR) finite at NLO, power-suppressed, and numerically small [39, 40], like the thermal mass of refs. [30, 31] which emerges as a part of these corrections [39]. However, as discussed around eq. (2.1) and eq. (3.4), these power-suppressed thermal corrections are in general not the dominant ones in the regime of eq. (2.3); thermal corrections exist which are only suppressed by the coupling, not by T^2/M^2 . In order to incorporate the dominant corrections close to threshold, both at $T = 0$ and at $T > 0$, a suitable resummed framework is needed.

Before proceeding to the resummed framework, it is appropriate to stress that the total annihilation rate from eq. (3.2) can be related to a purely Euclidean (imaginary-time) correlator [18]. Systematic higher-order perturbative computations and lattice studies should probably take the imaginary-time formulation as a starting point.

A way to compute resummed thermal spectral functions in the non-relativistic regime has been suggested in refs. [41, 42]. The power counting behind this framework has been discussed in great detail in ref. [43], and corresponds to eq. (2.3).⁶

Following eqs. (4.1)–(4.15) of ref. [42], the spectral function can be extracted from the imaginary part of a “Coulomb Green’s function”. This Green’s function satisfies an inhomogeneous Schrödinger-type equation, with the feature that the static potential contains a Debye-screened real part, as well as an imaginary part (Γ in the notation of sec. 2). The latter represents frequent thermal scatterings on light plasma constituents that decohere the DM particles. The processes are illustrated in fig. 2.

Let us define

$$E' \equiv \omega - 2M - \frac{k^2}{4M}, \quad (3.11)$$

where k is the momentum of the DM’-DM pair with respect to the heat bath (cf. eq. (3.8)). Through a slight abuse of notation we now redefine ρ to stand for the spectral function related to relative dynamics, $\rho(\omega, \mathbf{k}) \equiv \rho(E')$. A non-relativistic Hamiltonian is written as

$$H = -\frac{\nabla_r^2}{M} + V(r), \quad (3.12)$$

⁶Technically, the resummed framework assumes that the vacuum energy scale $\sim 2M$ and the thermal scale $\sim \pi T$ and certain other scales have been integrated out. Then M should be M_{th} as defined above eq. (3.5). In order to simplify the notation and because the thermal correction $\delta M_{\text{th}} = \Delta M_{\text{th}}^2/(2M)$ is numerically very small, we however keep the notation M for the heavy-particle mass in the following. In contrast, the Salpeter correction of eq. (2.1) is important; in our approach it emerges “dynamically” from the potential in eq. (3.24).

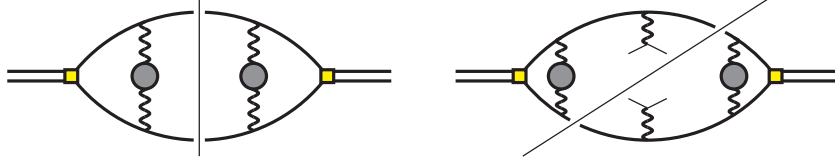


Figure 2: Processes incorporated through the solution of the Schrödinger equation, eq. (3.13), with a temperature-modified static potential, eq. (3.24). The thin line indicates a cut (i.e. an imaginary part, cf. eq. (3.14)). The complete solution includes an infinite re-iteration of both types of processes. Left: virtual corrections, originating from $V(r)$. Right: real corrections, originating from $\Gamma(r)$.

where $V(r)$ contains virtual corrections such as Debye screening and temperature-modified mixing angles. Then the spectral function is obtained from

$$[H - i\Gamma(r) - E']G(E'; \mathbf{r}, \mathbf{r}') = N\delta^{(3)}(\mathbf{r} - \mathbf{r}') , \quad (3.13)$$

$$\lim_{\mathbf{r}, \mathbf{r}' \rightarrow \mathbf{0}} \text{Im } G(E'; \mathbf{r}, \mathbf{r}') = \rho(E') , \quad (3.14)$$

where N is the number of degrees of freedom. Eq. (3.13) represents a Fourier transform of a time-dependent Schrödinger equation with a local source created at $t = 0$ and annihilated at time $t > 0$. The simplest realistic scenarios contain a complex scalar field or a non-relativistic fermionic spinor, for which $N = 2$. We note that in vacuum, i.e. by setting $\Gamma(r) \rightarrow 0^+$, the spectral function possesses the usual quantum-mechanical interpretation,

$$\lim_{T \rightarrow 0} \rho(E') = N \sum_m |\psi_m(\mathbf{0})|^2 \pi \delta(E_m - E') , \quad (3.15)$$

where E_m are the s -wave energy eigenvalues related to eq. (3.12) and ψ_m are the corresponding wave functions.

When expressed in the center-of-mass coordinates of eq. (3.11), the integral over k can be carried out in the Laplace transform of eq. (3.9). We get

$$\begin{aligned} \gamma &\approx \int_{\mathbf{k}} e^{-\frac{2M}{T} - \frac{k^2}{4MT}} \int_{-\Lambda}^{\infty} \frac{dE'}{\pi} e^{-E'/T} \rho(E') \\ &= \left(\frac{MT}{\pi}\right)^{3/2} e^{-2M/T} \int_{-\Lambda}^{\infty} \frac{dE'}{\pi} e^{-E'/T} \rho(E') . \end{aligned} \quad (3.16)$$

In the free limit, corresponding to $V(r) \rightarrow 0$ and $\Gamma \rightarrow 0^+$, eqs. (3.13) and (3.14) yield

$$\rho(E') \rightarrow \rho_{\text{free}}(E') \equiv \frac{NM^{\frac{3}{2}}\theta(E')\sqrt{E'}}{4\pi} . \quad (3.17)$$

Combining eqs. (3.16) and (3.17) and comparing with eq. (3.5), we get

$$\gamma_{\text{free}} \approx N \left[\left(\frac{MT}{2\pi}\right)^{3/2} e^{-M/T} \right]^2 \approx \frac{n_{\text{eq}}^2}{4N} . \quad (3.18)$$

A nice method to solve eqs. (3.13) and (3.14) is to reduce the solution of the inhomogeneous equation into the solution of the corresponding homogeneous equation which is regular at origin [44]. Let $\rho \equiv \alpha Mr$, $V \equiv \alpha^2 M \tilde{V}$, $\Gamma \equiv \alpha^2 M \tilde{\Gamma}$, $E' \equiv \alpha^2 M \tilde{E}'$, and denote by ℓ an angular quantum number. Then the radial homogeneous equation takes the form

$$\left[-\frac{d^2}{d\rho^2} + \frac{\ell(\ell+1)}{\rho^2} + \tilde{V} - i\tilde{\Gamma} - \tilde{E}' \right] u_\ell(\rho) = 0. \quad (3.19)$$

The regular solution is the one with the asymptotics $u_\ell = \rho^{\ell+1}$ at $\rho \ll 1$. With this normalization, the s -wave spectral function is obtained from

$$\rho(E') = \frac{\alpha N M^2}{4\pi} \int_0^\infty d\rho \operatorname{Im} \left[\frac{1}{(u_0)^2} \right]. \quad (3.20)$$

3.4. Resummed gauge field propagator and static potential

An essential role in the solution of eq. (3.19) is played by the static potential V and by its imaginary part, denoted by $-i\Gamma$. In typical DM models, $\lim_{T \rightarrow 0} V = -\alpha e^{-mr}/r$ and $\lim_{T \rightarrow 0} \Gamma = 0$. Then bound states exist if $M \gtrsim 1.6m/\alpha$ (cf., e.g., ref. [9]). In the regime where $\pi T \ll m$, thermal corrections are exponentially suppressed and bound states are not affected. Once $\pi T \sim m$, thermal corrections are of order unity, however they are rather complicated in this regime; we do *not* consider this situation. Rather, we go over to temperatures $\pi T \gg m$, which for Z boson exchange corresponds to $T \gg 30$ GeV. Even if πT is large compared with m , it is still small compared with M , which is assumed to satisfy $M \gtrsim 20T$.

In the regime $\pi T \gg m$, the gauge field self-energy obtains the so-called Hard Thermal Loop (HTL) form [27, 45–47] (for a derivation, see appendix A).⁷ This means that the gauge boson mass m is modified by a thermal correction of order gT , which is parametrically of the same order as m , or larger. The self-energy is in general momentum-dependent, however the relevant momentum scale is $k \sim m \ll \pi T$. Therefore momentum dependence is suppressed by $\sim k^2/(\pi T)^2 \ll 1$.

In a thermal system, several different self-energies can be defined, depending on the time ordering chosen. Only one choice can be consistently used in connection with eq. (3.19). Given that the DM'-DM pair is heavy and therefore behaves essentially as in vacuum, its interactions with gauge fields are encoded in a *time-ordered correlator*. For completeness we show this explicitly around eq. (7.14). At finite temperature this result has previously been established (directly or indirectly) in the context of QCD [29, 43] and QED [48].

The time-ordered propagator can be straightforwardly determined within the so-called imaginary-time formalism, in which the Feynman rules are identical to those in vacuum, apart from a Wick rotation. Then we compute an imaginary-time correlator, denoted by Δ_{00E} ,

⁷There are also HTL vertex corrections, but for heavy particles these can be omitted, cf. e.g. ref. [32].

for the temporal gauge field components with a Matsubara frequency k_n , and analytically continue it to obtain a retarded correlator,

$$\Delta_{00\text{R}} = \Delta_{00\text{E}}|_{k_n \rightarrow -i[\omega+i0^+]} . \quad (3.21)$$

Subsequently the time-ordered propagator reads (cf. e.g. refs. [49, 50])

$$i\Delta_{00\text{T}}(\omega, k) = \Delta_{00\text{R}}(\omega, k) + 2in_{\text{B}}(\omega) \text{Im} \Delta_{00\text{R}}(\omega, k) . \quad (3.22)$$

Given that for the static potential we are only interested in the static limit and that $n_{\text{B}}(\omega) \approx T/\omega$ for $\omega \ll T$, it is sufficient in practice to consider

$$i\Delta_{00\text{T}}(0, k) = \Delta_{00\text{R}}(0, k) + i \lim_{\omega \rightarrow 0} \frac{2T}{\omega} \text{Im} \Delta_{00\text{R}}(\omega, k) . \quad (3.23)$$

The static potential and the thermal width are obtained from (cf. sec. 7)

$$V(r) - i\Gamma(r) = g^2 C_{\text{R}} \int \frac{d^3\mathbf{k}}{(2\pi)^3} \left(1 - e^{i\mathbf{k}\cdot\mathbf{r}}\right) i\Delta_{00\text{T}}(0, k) - \delta V , \quad (3.24)$$

where we assume the counterterm δV to be so chosen that $\lim_{r \rightarrow \infty} V(r) = 0$ at $T = 0$.⁸ The \mathbf{r} -independent part originates from self-energy corrections and the \mathbf{r} -dependent one from exchange contributions, and C_{R} is a Casimir factor.

The real and imaginary parts of the gauge field propagator, eq. (3.23), lead to specific physical phenomena which have been illustrated in fig. 2. The real part corresponds to “virtual exchange”, i.e. a Debye screened potential. The imaginary part corresponds to “real scatterings”, specifically the scattering of the heavy particles on light plasma constituents; its physical origin is reiterated in eqs. (A.11) and (A.12). For $r \rightarrow \infty$, $V(\infty)$ corresponds to twice the heavy particle thermal mass correction (cf. eq. (2.1)), and $\Gamma(\infty)$ to twice the heavy particle thermal interaction rate [27, 48]. The interpretation of Γ in the language of open quantum systems has been discussed in ref. [51]. Finally, we recall that the Bose-enhanced term in eq. (3.23), representing large occupation numbers $\sim T/\omega \gg 1$, has a classical plasma physics interpretation: electric fields exert a Lorentz force on charged particles, which induces a current, by which the electric field is reduced. In the real-time formalism, the Bose-enhanced contribution originates from the rr -propagator in the r/a basis, and gives the dominant contribution to typical soft observables [52].

3.5. Summary of the theoretical framework

We have argued that the computation of massive dark matter relic density can be factorized into a number of independent steps. First, the thermal self-energies of the particles exchanged

⁸More precisely, a counterterm is needed because the self-energy correction is linearly ultraviolet divergent in vacuum. Its finite part defines what we mean by the renormalized heavy-particle mass M .

by the dark ones need to be computed. From the self-energies, the corresponding propagators can be determined (cf. eq. (3.23)). These fix the static potential and the thermal width experienced by the annihilating pair (cf. eq. (3.24)). Subsequently the spectral function can be computed through the solution of a Schrödinger equation (cf. eqs. (3.13) and (3.14)). Its Laplace-transform gives the thermally averaged annihilation rate (cf. eq. (3.16)). The annihilation rate parametrizes a rate equation, which can be integrated to give the final non-equilibrium number density (cf. eq. (3.1) or (3.3)). In principle the uncertainties of each of these steps can be scrutinized and improved upon separately.

4. Z exchange at finite temperature

Our first physics goal is to apply the formalism of sec. 3 to determine the spectrum of a kinetically equilibrated DM' -DM pair interacting through Z boson exchange. Non-relativistic particles interacting with Z bosons are represented either by a complex scalar field or by a two-component spinor, and in general the two degrees of freedom have different masses. Here we focus on a case in which the two degrees of freedom are degenerate in mass; the non-degenerate case is addressed in sec. 7.

With this setup, the parameters defined in sec. 3.4 are

$$\alpha \equiv \frac{g_1^2 + g_2^2}{16\pi} \approx 0.01, \quad m \equiv m_Z \approx 91 \text{ GeV}, \quad (4.1)$$

where g_1 and g_2 are the hypercharge and weak gauge couplings, respectively. Solving a static Schrödinger equation with a Yukawa potential with these parameters, a $1s$ bound state is found for $M \gtrsim 15$ TeV. Here we consider $M \lesssim 10$ TeV so that no bound states exist.⁹

The general forms of the self-energies and propagators needed for Z exchange are reviewed in appendix A. Here we proceed with the propagator from eq. (A.24). We denote the vacuum and thermal mixing angles by θ and $\tilde{\theta}$, where [53]

$$\sin(2\theta) \equiv \frac{2g_1g_2}{g_1^2 + g_2^2}, \quad (4.2)$$

$$\sin(2\tilde{\theta}) \equiv \frac{\sin(2\theta)m_Z^2}{\sqrt{\sin^2(2\theta)m_Z^4 + [\cos(2\theta)m_Z^2 + m_{E2}^2 - m_{E1}^2]^2}}. \quad (4.3)$$

The $U_Y(1)$ and $SU_L(2)$ Debye masses read [54]

$$m_{E1}^2 \equiv \left(\frac{n_S}{6} + \frac{5n_G}{9}\right)g_1^2T^2, \quad m_{E2}^2 \equiv \left(\frac{2}{3} + \frac{n_S}{6} + \frac{n_G}{3}\right)g_2^2T^2, \quad (4.4)$$

⁹For completeness we note that if $M \gtrsim 15$ TeV, bound states exist but they melt at temperatures below the thermal freeze-out, in analogy with the case of Z' exchange considered in fig. 4.

where $n_S \equiv 1$ and $n_G \equiv 3$ are the numbers of Higgs doublets and fermion generations, respectively. The neutral eigenstates have the masses

$$m_{\tilde{Z}}^2 \equiv m_+^2, \quad m_{\tilde{Q}}^2 \equiv m_-^2, \quad (4.5)$$

$$m_{\pm}^2 \equiv \frac{1}{2} \left\{ m_Z^2 + m_{E1}^2 + m_{E2}^2 \pm \sqrt{\sin^2(2\theta)m_Z^4 + [\cos(2\theta)m_Z^2 + m_{E2}^2 - m_{E1}^2]^2} \right\}. \quad (4.6)$$

Then the potential from eq. (3.24), fixing δV from $\lim_{r \rightarrow \infty} \lim_{T \rightarrow 0} V(r) = 0$, takes the form

$$V(r) \approx \alpha \left\{ m_Z^{(T=0)} - \cos^2(\tilde{\theta} - \theta) \left[m_{\tilde{Z}} + \frac{\exp(-m_{\tilde{Z}}r)}{r} \right] - \sin^2(\tilde{\theta} - \theta) \left[m_{\tilde{Q}} + \frac{\exp(-m_{\tilde{Q}}r)}{r} \right] \right\}, \quad (4.7)$$

whereas the imaginary part can be expressed as

$$\begin{aligned} \Gamma(r) \approx \alpha T \left\{ \frac{\cos^2(\tilde{\theta} - \theta)(m_{E1}^2 \sin^2 \tilde{\theta} + m_{E2}^2 \cos^2 \tilde{\theta}) \phi(m_{\tilde{Z}}r)}{m_{\tilde{Z}}^2} \right. \\ + \frac{\sin^2(\tilde{\theta} - \theta)(m_{E1}^2 \cos^2 \tilde{\theta} + m_{E2}^2 \sin^2 \tilde{\theta}) \phi(m_{\tilde{Q}}r)}{m_{\tilde{Q}}^2} \\ \left. + \frac{\sin(2(\tilde{\theta} - \theta)) \sin(2\tilde{\theta})(m_{E2}^2 - m_{E1}^2) \theta(m_{\tilde{Z}}r, m_{\tilde{Q}}r)}{2(m_{\tilde{Z}}^2 - m_{\tilde{Q}}^2)} \right\}. \end{aligned} \quad (4.8)$$

Here we have defined

$$\phi(\rho) \equiv 1 - 2 \int_0^\infty \frac{dx}{(x^2 + 1)^2} \frac{\sin(x\rho)}{\rho}, \quad (4.9)$$

$$\theta(\rho_1, \rho_2) \equiv 2 \ln\left(\frac{\rho_1}{\rho_2}\right) + 2 \int_0^\infty \frac{dx}{x^2 + 1} \left[\frac{\sin(x\rho_1)}{\rho_1} - \frac{\sin(x\rho_2)}{\rho_2} \right], \quad (4.10)$$

both of which vanish at zero separation ($r \rightarrow 0$).

We consider a semi-realistic choice for the dark matter mass scale, $M \gtrsim 1$ TeV. As alluded to above, the lower bound is dictated by the ease of computation, but phenomenological constraints from the LHC favour a similar value. Results are shown in fig. 3. The thermal scatterings experienced by the DM particles with light plasma constituents (cf. fig. 2) cause the 2-particle threshold to smoothen, but the most important effect is related to Debye screening, both through the shift of the threshold location according to the Salpeter correction from eq. (2.1) and through modified Sommerfeld factors, as we now explain.

In fig. 3 we show with a solid line the result corresponding to a Sommerfeld factor for attractive Coulomb exchange. This can be expressed as [24]

$$S = \frac{X}{1 - e^{-X}}, \quad X = \frac{\pi\alpha}{v}, \quad (4.11)$$

where E' from eq. (3.11) has been parametrized through a velocity as $E' = Mv^2$. We use the Coulomb form, because for $M \gtrsim 3$ TeV electroweak symmetry is restored around the freeze-out temperature. The main difference from the Coulomb case is due to Debye screening (cf.

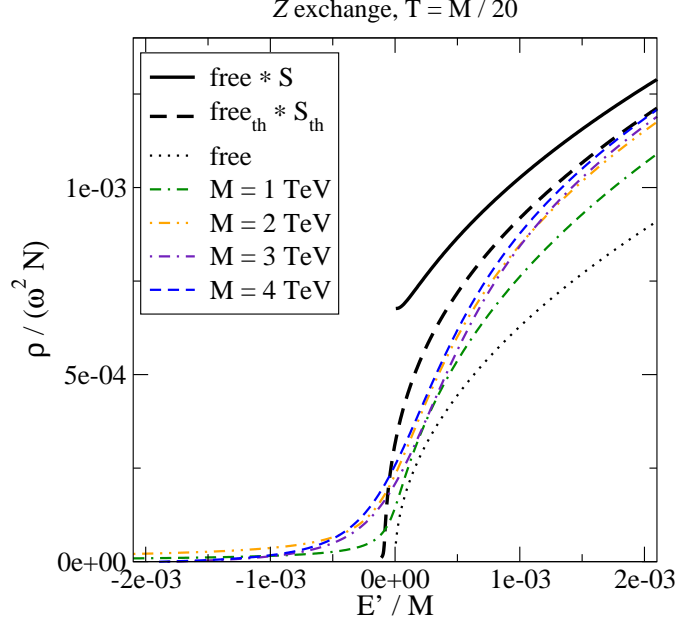


Figure 3: The free (dotted line; cf. eq. (3.17)) and resummed (coloured lines; cf. eq. (3.20)) spectral functions, with E' denoting the energy with respect to the 2-particle threshold and $\omega \equiv 2M + E'$. The potential and width are from eqs. (4.7) and (4.8), respectively. The free result multiplied by the Sommerfeld factor S from eq. (4.11) is shown with a solid line. We also display a numerically determined Sommerfeld factor which includes the effects of Debye screening and a shift of the threshold location according to the Salpeter correction from eq. (2.1) ($\text{free}_{\text{th}} * S_{\text{th}}$; $M = 3$ TeV).

eq. (4.4)), which persists at high temperatures. The numerically determined Debye-screened Sommerfeld factor has been illustrated in fig. 3 with a dashed line, and agrees well with the full solution soon above the threshold.

The total annihilation rate γ is given by the Laplace transform in eq. (3.16). Given that $M/T \sim 20 \dots 25$, the Laplace transform corresponds to an average over the range $E'/M \lesssim 0.1$. This is a broad range in comparison with the threshold region $|E'| \lesssim 20\alpha^2 M$ shown in fig. 3. In particular, the suppression with respect to the Debye-screened Sommerfeld prediction at $E' > 0$ is largely compensated for by the enhanced spectral weight at $E' < 0$. Moreover, the suppression of the Sommerfeld factor by Debye screening amounts to a higher-order correction to the total rate. The shift of the threshold location to the left increases the annihilation rate according to eq. (2.1), but the suppression of the Sommerfeld factor by Debye screening decreases it; we find that the final result for γ is $\sim 1\%$ below the Coulombic Sommerfeld estimate.¹⁰ The enhancement with respect to the free result is $\sim 9\%$.

¹⁰Thermal corrections were anticipated to be small in ref. [55], however only some of them were included.

5. Z' exchange at finite temperature

For a further illustration we move on to a technically simpler model, similar to those for which “wimponium” bound states were found at zero temperature [6–9]. More specifically, we consider a dark sector with an U(1) gauge symmetry, coupled to the Standard Model through a vector or Higgs portal (cf. e.g. refs. [56–58]). Being only interested in qualitative features the portal couplings will be omitted for practical purposes, apart from assuming that the dark sector is in kinetic equilibrium with the Standard Model. The dark sector then consists of the heavy dark matter particle (ψ), the dark gauge boson (V_μ), and a dark Higgs field (S) which gives the dark gauge boson a mass $m_V \gtrsim 1$ GeV as is required for phenomenology (cf. e.g. refs. [59, 60]). We refer to the dark gauge boson as Z' .

A concrete realization of the above setup is provided by the Lagrangian

$$\mathcal{L} = \mathcal{L}_{\text{SM}} + \mathcal{L}_{\text{portal}} - \frac{1}{4} V^{\mu\nu} V_{\mu\nu} + (D^\mu S)^* (D_\mu S) - V(S^* S) + \bar{\psi} (i\gamma^\mu D_\mu - M) \psi, \quad (5.1)$$

where $V_{\mu\nu}$ is the field strength corresponding to the dark U(1). The potential breaks the U(1) gauge symmetry spontaneously, $V(S^* S) \simeq -\nu^2 S^* S + \lambda' (S^* S)^2$, $\nu^2, \lambda' > 0$. Portal couplings have the form $\mathcal{L}_{\text{portal}} = -\kappa_1 V^{\mu\nu} F_{\mu\nu} - \kappa_2 S^* S H^\dagger H$, where $F_{\mu\nu}$ is the Standard Model hypercharge field strength and H is the Higgs doublet. Both κ_1 and κ_2 are assumed small enough to be insignificant in practice. The coupling associated with the dark U(1) group is denoted by e' , and $D_\mu = \partial_\mu - ie' V_\mu$. In accordance with ref. [6], in which the phenomenology of this model was discussed, we take $\alpha' \equiv (e')^2/(4\pi) \sim 0.01$. The mass of the scalar particle is assumed to be $m_S \sim 1$ GeV but it plays little role. Dark matter particles with $M \sim \text{TeV}$ freeze out in the non-relativistic regime as usual. For these parameters the constraint $M \gtrsim 1.6 m_V / \alpha'$ (cf., e.g., ref. [9]) is well satisfied, guaranteeing the existence of bound states in vacuum.

A computation of the Z' self-energy in this model is presented in appendix B. Defining a thermally modified Z' mass as

$$m_{\tilde{V}}^2 \equiv m_V^2 + m_{\text{E}'}^2, \quad m_V'^2 \equiv e'^2 v_T'^2, \quad m_{\text{E}'}^2 \equiv \frac{e'^2 T^2}{3}, \quad (5.2)$$

where v_T' is the thermal expectation value of S ($S = v_T'/\sqrt{2} + \dots$), and choosing δV so that $\lim_{r \rightarrow \infty} V(r) = 0$ at $T = 0$, eqs. (B.4) and (3.24) yield

$$V(r) \approx \alpha' \left\{ m_V^{(T=0)} - \left[m_{\tilde{V}} + \frac{\exp(-m_{\tilde{V}} r)}{r} \right] \right\}, \quad \Gamma(r) \approx \frac{\alpha' T m_{\text{E}'}^2 \phi(m_{\tilde{V}} r)}{m_{\tilde{V}}^2}. \quad (5.3)$$

Here the function ϕ is from eq. (4.9). The spectral function is determined from eqs. (3.19) and (3.20). Given that $\pi T \gg m_V$, the mass m_V is insignificant in practice; in fact the dark U(1) symmetry is restored at the temperatures at which freeze-out takes place.

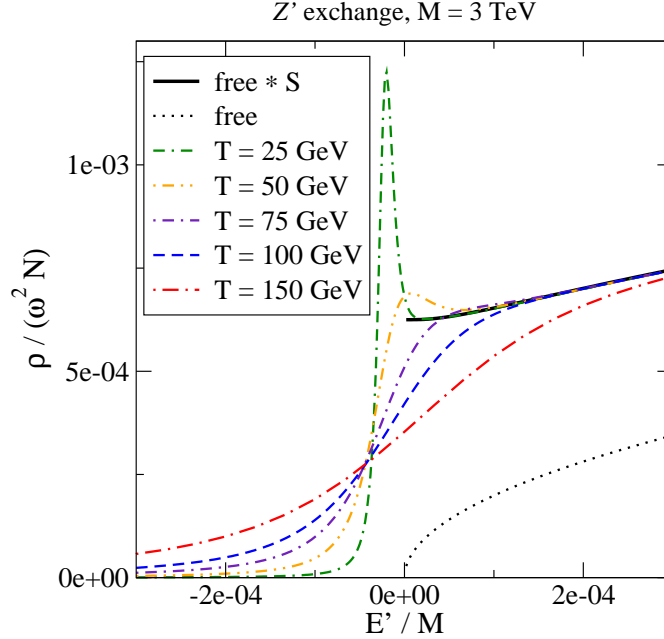


Figure 4: The free, Sommerfeld enhanced, and resummed spectral functions for Z' exchange, for $M = 3$ TeV and $N = 2$ and the potential and width from eq. (5.3). The notation is as in fig. 3.

Illustrative results for $M = 3$ TeV are shown in fig. 4. The bound state peak is found to dissolve at a temperature $T \sim 75$ GeV, i.e. below freeze-out, $T_{\text{freeze-out}} \gtrsim 100$ GeV. The spectral function gets smoothened across the threshold. Around $T_{\text{freeze-out}}$ the physical annihilation rate obtained from the Laplace transform in eq. (3.16) is however in good agreement with that predicted by the Sommerfeld factor.

6. Gluon exchange at finite temperature

Let us turn to strong interactions. In the context of supersymmetric theories, one scenario that has attracted interest is the case of neutralino dark matter, which could co-annihilate with gluinos just slightly heavier than neutralinos. The gluinos themselves may form bound states, which also annihilate. This system has been analyzed within a Boltzmann equation approach in, for instance, refs. [14,61]. (Much the same could be done if gluinos were replaced by stops, cf. e.g. refs. [62–64] and references therein.)

For the purposes of the present paper, we only consider the gluino part of the set of non-equilibrium variables.¹¹ The question is whether gluino bound states can persist up to high

¹¹The full set of dark matter rate equations necessitates a non-trivial discussion in the co-annihilation regime, implying in particular that the gluino annihilation rate contributes to an effective $\langle\sigma v\rangle$ with a certain weight but is not the only ingredient [1]. For simplicity we discuss here only the gluino annihilation rate.

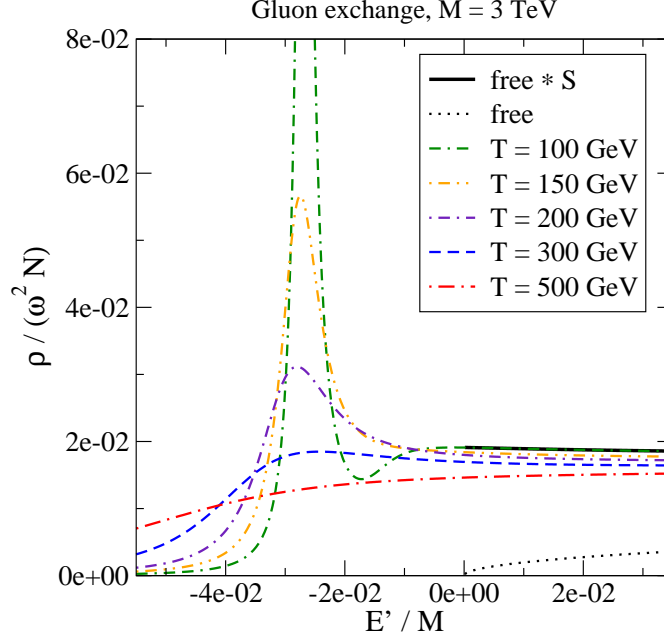


Figure 5: The free and resummed spectral functions for gluon exchange, with $M = 3$ TeV and $N = 16$. The potential and width are from eq. (6.2). The notation is as in fig. 3. The Sommerfeld factor S was computed for $T = 100$ GeV.

temperatures and, if so, how strongly they would affect the gluino annihilation rate.

For the case of gluon exchange, the results for the real-time static potential can be taken over from QCD literature [29, 43, 48], with a simple change of group theory factors. Defining the Debye mass and an effective coupling for the adjoint matter representation as

$$m_{\text{E}3}^2 \equiv \left(1 + \frac{n_G}{3}\right) g_3^2 T^2, \quad \alpha_3 \equiv \frac{3g_3^2}{4\pi}, \quad (6.1)$$

where $n_G = 3$ is the number of generations and $g_3^2 \equiv 4\pi\alpha_s$, and concentrating on the attractive interaction in the singlet channel like in ref. [14], we get

$$V(r) \approx -\alpha_3 \left[m_{\text{E}3} + \frac{\exp(-m_{\text{E}3} r)}{r} \right], \quad \Gamma(r) \approx \alpha_3 T \phi(m_{\text{E}3} r), \quad (6.2)$$

where ϕ is from eq. (4.9). Here $V(\infty)$ and $\Gamma(\infty)$ correspond to a thermal mass correction (cf. eq. (2.1)) and interaction rate [27] of two independent heavy gluinos.

The result of this procedure is shown in fig. 5, for $M = 3$ TeV. At $T = M/20 = 150$ GeV, a bound state is clearly visible, and at $T = M/25$ even more so. If the gluino is substantially heavier than the DM particle then, for a given gluino mass M , the freeze-out temperature would be lower than $M/25$, and bound states would be very prominent.

Once the temperature is high enough, bound states do dissolve even with strong interactions. For instance, the curve $T = 500$ GeV in fig. 5 only shows a broad gradually rising

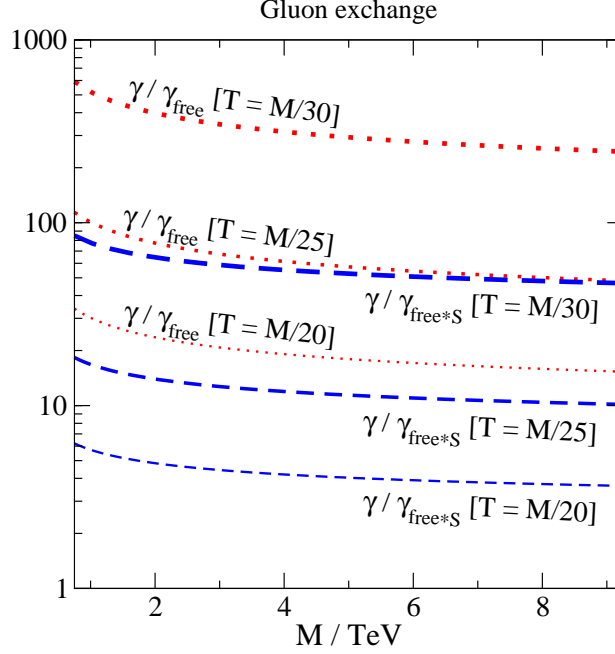


Figure 6: The ratio of the total rate from eq. (3.16) to the rates obtained from the approximations “free” and “free * S ”, where S denotes the Sommerfeld factor. The spectral function originates from gluon exchange and was illustrated in fig. 5. The total rate exceeds the Sommerfeld estimate by a factor $\sim 4 \dots 80$, and the free rate by $15 \dots 600$, depending on parameter values.

spectral shape. Its general position is shifted to the left of the free threshold because of the Salpeter correction discussed below eq. (2.1). Because of frequent elastic scatterings with plasma particles, which decohere any sharp quantum-mechanical features, the spectral function is a smooth function. Bound states have disappeared because of two reasons: Debye screening makes the potential less binding [17] and, already at a lower temperature, the thermal interaction rate (or width) caused by the frequent elastic scatterings becomes larger than the binding energy of any of the bound states [33–35].

Integrating over the spectral function with the Boltzmann weight yields the total annihilation rate, cf. eq. (3.16). The corresponding results are shown in fig. 6, in comparison with results obtained from non-interacting ($\equiv \gamma_{\text{free}}$) and Sommerfeld-enhanced ($\equiv \gamma_{\text{free}*S}$) computations. Compared with the Sommerfeld-enhanced computation, the bound state contribution boosts the annihilation rate by a factor $4 \dots 80$, depending on parameter values.

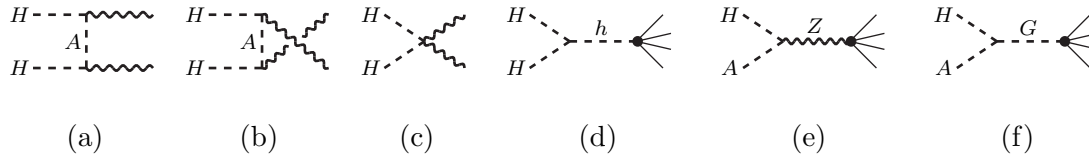


Figure 7: Examples of how dark matter particles described by the model of eq. (7.1) can get annihilated. Wiggly lines stand for Z bosons and thin solid lines for generic Standard Model particles. The operators of eq. (7.6) originate from processes (a)–(c) and their interference terms. Process (d) mediated by the Higgs boson h and its interference with (a)–(c) is numerically important (cf. e.g. ref. [65]) but leads to no new operators. All the reactions also take place with the exchange $H \leftrightarrow A$. Process (e) leads to a p -wave operator or to effects suppressed by the mass difference $(\Delta M)^2$; the latter type can also originate from process (f) mediated by a Goldstone mode G .

7. Non-degenerate masses

We now proceed to cases, relevant e.g. for weak interactions, in which the particles interacting through gauge exchange are non-degenerate in mass. We denote the mass difference by ΔM . If ΔM originates from a Higgs mechanism, we expect it to be “small” in general, $\Delta M \lesssim m_Z$. We work in a regime $m_Z \ll \pi T$ (cf. sec. 3.4). Then $\Delta M \ll \pi T \ll M$, and the effects of ΔM can be incorporated within a non-relativistic framework. Our goal is to show that having $\Delta M > 0$ changes the situation only “smoothly” compared with the degenerate case. To this end we consider a simple model and carry out a quantum-statistical computation of correlators of the type illustrated in fig. 1.

7.1. A model and its non-relativistic description

Consider a dark sector consisting of an additional Higgs doublet. In the presence of electroweak symmetry breaking, there are four physical states in this sector, the neutral ones denoted by H and A and two charged ones denoted by H^\pm . For simplicity we consider a situation in which $m_{H^\pm} \gg m_H, m_A$. The state H is taken to be the lightest particle ($M \equiv m_H$) and A is slightly heavier ($\Delta M \equiv m_A - m_H > 0$). The Lagrangian describing the interactions of these fields with physical Z bosons reads

$$\mathcal{L} \equiv \frac{1}{2} D_\mu^* (H + iA) D^\mu (H - iA) - \frac{1}{2} m_H^2 H^2 - \frac{1}{2} m_A^2 A^2 + \dots, \quad (7.1)$$

where $D_\mu \equiv \partial_\mu + igZ_\mu$ and $g \equiv \frac{1}{2}\sqrt{g_1^2 + g_2^2}$. There are also interactions with the Higgs boson (cf. fig. 7(d)) but these do not change the qualitative behaviour, so we omit them here.

For a transparent discussion, it is helpful to go over into a non-relativistic Hamiltonian

description. The interaction part of eq. (7.1) reads

$$\mathcal{L}_{\text{int}} = gZ^\mu (A \partial_\mu H - H \partial_\mu A) + \frac{g^2}{2} Z^\mu Z_\mu (H^2 + A^2) + \dots \quad (7.2)$$

Key steps of the argument can be simplified by assuming the scalar fields H and A to be so heavy that they are essentially static; then they can be described by the non-relativistic modes ϕ and χ as

$$H \simeq \frac{1}{\sqrt{2m_H}} \left(\phi e^{-im_H t} + \phi^\dagger e^{im_H t} \right), \quad A \simeq \frac{1}{\sqrt{2m_A}} \left(\chi e^{-im_A t} + \chi^\dagger e^{im_A t} \right). \quad (7.3)$$

Inserting these decompositions into eq. (7.2); taking the limit $m_H, m_A \sim M \gg m_Z, \Delta M$; and defining subsequently an interaction Hamiltonian as $\mathcal{H}_{\text{int}} \equiv -\mathcal{L}_{\text{int}}$, we get

$$\mathcal{H}_{\text{int}} = igZ_0 \left(\chi^\dagger \phi e^{i\Delta M t} - \phi^\dagger \chi e^{-i\Delta M t} \right) + \mathcal{O}\left(\frac{1}{M}\right). \quad (7.4)$$

It is furthermore convenient to employ Euclidean (imaginary-time) conventions for Z_0 , i.e. $Z_0^M = iZ_0^E$; we use Z_0^E in the following, without displaying the superscript. Thereby the interaction Hamiltonian between the static scalar fields and Z bosons becomes

$$H_{\text{int}}(t) = -g \int_{\mathbf{x}} Z_0(t, \mathbf{x}) \left[(\chi^\dagger \phi)(\mathbf{x}) e^{i\Delta M t} - (\phi^\dagger \chi)(\mathbf{x}) e^{-i\Delta M t} \right] + \mathcal{O}\left(\frac{1}{M}\right). \quad (7.5)$$

Next, we need the four-particle operators describing the annihilations of H and A . Examples of processes are illustrated in fig. 7. Considering only effects from the gauge vertices in eq. (7.1), processes (a)–(c) and their interference terms yield an imaginary four-particle operator in the sense of ref. [20],

$$\delta\mathcal{L}_{\text{eff}} \simeq \frac{ig^4}{64\pi} \left(\frac{\phi^\dagger \phi^\dagger \phi \phi}{m_H^2} + \frac{\chi^\dagger \chi^\dagger \chi \chi}{m_A^2} \right). \quad (7.6)$$

7.2. Derivation of a real-time static potential

Now, in accordance with the discussion in sec. 3.2, the role of eq. (7.6) is that it dictates the spectral functions which need to be determined. In the language of eq. (3.8), two spectral functions play a role: one in which we replace $\eta\theta \rightarrow \phi\phi$, $\theta^\dagger\eta^\dagger \rightarrow \phi^\dagger\phi^\dagger$; another in which $\eta\theta \rightarrow \chi\chi$, $\theta^\dagger\eta^\dagger \rightarrow \chi^\dagger\chi^\dagger$. Furthermore, as suggested by fig. 1(a), the Schrödinger equation determining the spectral functions induces a mixing between the two channels.

In order to determine the mixing, we consider a quantum-mechanical problem with the interaction Hamiltonian in eq. (7.5). Let us define the Wightman function

$$C_{>}(t) \equiv \text{Tr} \left\{ \hat{\rho} \left[\chi(\mathbf{r}) \chi(\mathbf{0}) U_I(t; 0) \phi^\dagger(\mathbf{r}) \phi^\dagger(\mathbf{0}) \right] \right\}, \quad (7.7)$$

which corresponds to “half” of the process in fig. 1(a). Here U_I is the time evolution operator in the interaction picture. The density matrix $\hat{\rho}$ is assumed to have the form $\hat{\rho} \equiv \mathcal{Z}_0^{-1} e^{-H_0/T} \otimes$

$|0\rangle\langle 0|$, where H_0 is the Hamiltonian of the Standard Model and $|0\rangle$ is the vacuum state in the sector of the Hilbert space containing the dark particles. The time evolution operator can be expanded as usual,

$$U_I(t; 0) = \mathbb{1} - i \int_0^t dt_1 H_{\text{int}}(t_1) - \int_0^t dt_1 \int_0^{t_1} dt_2 H_{\text{int}}(t_1) H_{\text{int}}(t_2) + \mathcal{O}(g^3) . \quad (7.8)$$

The heavy particles can be dealt with by making use of canonical commutation relations, $[\phi(\mathbf{x}), \phi^\dagger(\mathbf{y})] = \delta^{(3)}(\mathbf{x} - \mathbf{y})$, etc. Thereby a non-zero contraction is obtained which contains the gauge correlator

$$\mathcal{V}_{\chi\phi}(t) \equiv -g^2 \int_0^t dt_1 \int_0^{t_1} dt_2 e^{i\Delta M(t_1+t_2)} \left\langle Z_0(t_1, \mathbf{r}) Z_0(t_2, \mathbf{0}) + Z_0(t_1, \mathbf{0}) Z_0(t_2, \mathbf{r}) \right\rangle , \quad (7.9)$$

where $\langle \dots \rangle$ denotes a thermal average with the density matrix $\mathcal{Z}_0^{-1} e^{-H_0/T}$. We can symmetrize the integrand in $t_1 \leftrightarrow t_2$ by introducing a time-ordered correlator, $\langle \dots \rangle_{\text{T}}$. Furthermore, assuming parity symmetry, the Z_0 propagator can be written as an inverse Fourier transform,

$$\frac{1}{2} \left\langle Z_0(t_1, \mathbf{r}) Z_0(t_2, \mathbf{0}) + Z_0(t_1, \mathbf{0}) Z_0(t_2, \mathbf{r}) \right\rangle_{\text{T}} = \int_{\omega, \mathbf{k}} e^{-i\omega(t_1-t_2) + i\mathbf{k}\cdot\mathbf{r}} \langle Z_0 Z_0 \rangle_{\text{T}}(\omega, k) . \quad (7.10)$$

Subsequently the time integrals can be carried out:

$$\Phi(t) \equiv \int_0^t dt_1 \int_0^{t_1} dt_2 e^{i\Delta M(t_1+t_2) - i\omega(t_1-t_2)} = e^{i\Delta M t} \frac{2 \sin\left[\frac{(\omega+\Delta M)t}{2}\right]}{\omega + \Delta M} \frac{2 \sin\left[\frac{(\omega-\Delta M)t}{2}\right]}{\omega - \Delta M} . \quad (7.11)$$

Recalling that $\lim_{t \rightarrow \infty} \frac{\sin(xt)}{x} = \pi \delta(x)$, we see that eq. (7.11) is proportional to $\delta(\omega + \Delta M) \delta(\omega - \Delta M)$ for $t \rightarrow \infty$. It thus yields a vanishing contribution if $\Delta M > 0$. This is a reflection of the fact that with non-degenerate masses and strictly static on-shell states the process in fig. 1(a) violates energy conservation.

Of course, the heavy particles are not exactly static, but can move (this is illustrated in fig. 1(a)). This permits for the exchange contribution to play a role. A way to determine its magnitude is to think of ΔM as a low-energy parameter, and to view the computation above as a high-energy matching step. The matching computation can most simply be carried out in the limit $\Delta M \rightarrow 0$, whereby eq. (7.11) becomes

$$\lim_{\Delta M \rightarrow 0} \Phi(t) = \frac{4 \sin^2\left(\frac{\omega t}{2}\right)}{\omega^2} . \quad (7.12)$$

Now we obtain a non-vanishing distribution in the large- t limit,

$$\lim_{t \rightarrow \infty} i \partial_t \left\{ \lim_{\Delta M \rightarrow 0} \Phi(t) \right\} = \lim_{t \rightarrow \infty} \frac{2i \sin(\omega t)}{\omega} = 2\pi i \delta(\omega) . \quad (7.13)$$

Therefore the potential from eq. (7.9) carries non-zero energy,

$$\lim_{t \rightarrow \infty} i \partial_t \left\{ \lim_{\Delta M \rightarrow 0} \mathcal{V}_{\chi\phi}(t) \right\} = -g^2 \int_{\mathbf{k}} e^{i\mathbf{k}\cdot\mathbf{r}} i \langle Z_0 Z_0 \rangle_{\text{T}}(0, k) . \quad (7.14)$$

This is like the \mathbf{r} -dependent part of eq. (3.24), but now the contribution mixes two different channels. Such a “non-diagonal” potential was included, e.g., in the analysis of ref. [66].

A similar computation yields also self-energy contributions ($\chi \rightarrow \phi$ in eq. (7.7)), originating from the “crossed terms” in two appearances of H_{int} in eq. (7.8):

$$\lim_{t \rightarrow \infty} i \partial_t \left\{ \lim_{\Delta M \rightarrow 0} \mathcal{V}_{\phi\phi}(t) \right\} = g^2 \int_{\mathbf{k}} i \langle Z_0 Z_0 \rangle_{\text{T}}(0, k) . \quad (7.15)$$

This is the \mathbf{r} -independent part of eq. (3.24). Recalling the vacuum counterterm δV and the form of the propagator in eq. (3.23) and noting that $\int_{\mathbf{k}} (\frac{1}{k^2 + m_{\text{th}}^2} - \frac{1}{k^2}) = -m_{\text{th}}/(4\pi)$, the real part of eq. (7.15) amounts to the Salpeter correction discussed around eq. (2.1)

Finally, it is amusing to consider the process shown in fig. 1(b), which plays a role in the annihilations shown in figs. 7(e) and (f). The relevant Wightman function now reads

$$D_{>}(t) \equiv \text{Tr} \left\{ \hat{\rho} \left[\phi(\mathbf{0}) \chi(\mathbf{r}) U_I(t; 0) \phi^\dagger(\mathbf{r}) \chi^\dagger(\mathbf{0}) \right] \right\} . \quad (7.16)$$

A non-zero contribution originates from the crossed terms in the product $H_{\text{int}}(t_1) H_{\text{int}}(t_2)$, cf. eq. (7.5). For $\Delta M \neq 0$ the time dependence is different from that in eq. (7.11), however for $\Delta M \rightarrow 0$ it is the same and a potential emerges like in eq. (7.14). The overall sign is positive, representing a repulsive interaction in this channel, suppressing such annihilations.

7.3. Numerical results

In the presence of the mixing from eq. (7.14) and assuming $\Delta M \ll M$, the equations to be solved amount to a matrix version of eq. (3.13),

$$\begin{pmatrix} H_{\phi\phi} - i\Gamma_{\phi\phi} - E' & V_{\phi\chi} - i\Gamma_{\phi\chi} \\ V_{\chi\phi} - i\Gamma_{\chi\phi} & 2\Delta M + H_{\chi\chi} - i\Gamma_{\chi\chi} - E' \end{pmatrix} \begin{pmatrix} G_\phi \\ G_\chi \end{pmatrix} = \begin{pmatrix} \delta^{(3)}(\mathbf{r} - \mathbf{r}') \\ \delta^{(3)}(\mathbf{r} - \mathbf{r}') \end{pmatrix} , \quad (7.17)$$

where $H_{\phi\phi} = -\nabla^2/M + V_{\phi\phi}$; $V_{\phi\phi} = V_{\chi\chi}$ is the r -independent part of eq. (4.7); $V_{\phi\chi} = V_{\chi\phi}$ is the r -dependent part of eq. (4.7); $\Gamma_{\phi\phi} = \Gamma_{\chi\chi}$ is $\Gamma(\infty)$ from eq. (4.8); and $\Gamma_{\phi\chi} = \Gamma_{\chi\phi}$ is $\Gamma(r) - \Gamma(\infty)$ from eq. (4.8). Two separate spectral functions are obtained from eq. (3.20),

$$\rho_\phi \equiv \frac{\alpha M^2}{4\pi} \int_0^\infty d\rho \text{Im} \left[\frac{1}{(u_0^\phi)^2} \right] , \quad \rho_\chi \equiv \frac{\alpha M^2}{4\pi} \int_0^\infty d\rho \text{Im} \left[\frac{1}{(u_0^\chi)^2} \right] . \quad (7.18)$$

In a vacuum limit these correspond to $\sum_m |\psi_m(\mathbf{0}; \pm)|^2 \pi \delta(E_m - E')$, respectively, where \pm denote the upper and lower “spin” components (ϕ and χ).

The physics of this system is subtle for $E' \lesssim 2\Delta M$. In this regime, the χ -pairs can only appear as “virtual” particles. One can imagine that they are “integrated out”; it can be shown that this generates an attractive potential for the ϕ -pair. Considering $\Delta M = 3\alpha^2 M$ as an example, we have solved the equations for two cases: the correct Debye-screened potentials

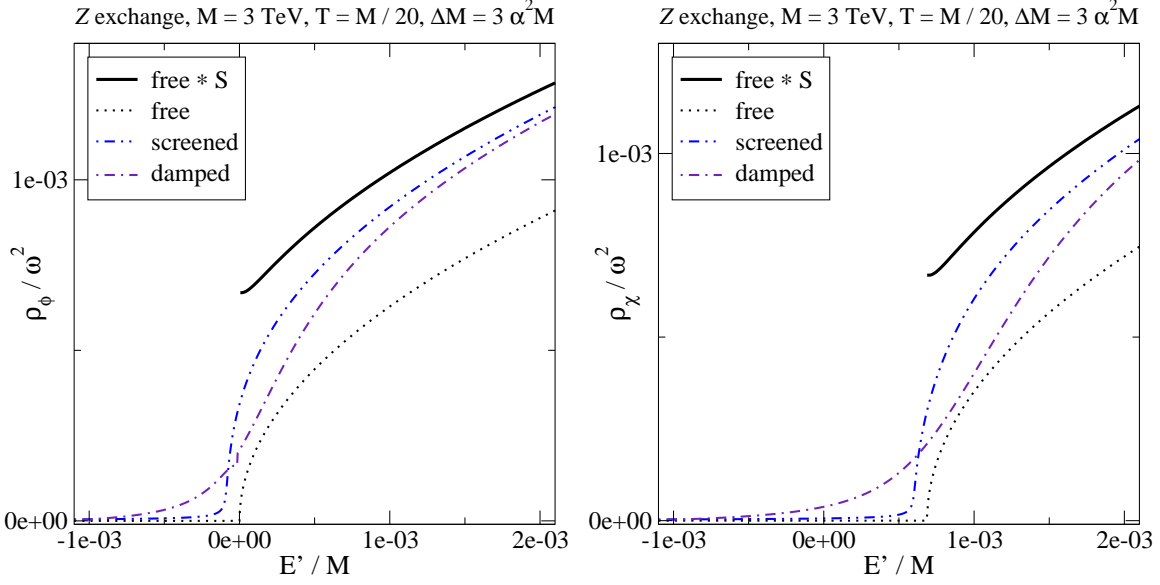


Figure 8: Spectral functions obtained from eqs. (7.17) and (7.18). Left: ρ_ϕ . Right: ρ_χ . By “screened” we denote thermal V ’s but omitting Γ ’s, and by “damped” the full system. In the former case, small imaginary parts $\Gamma_{\phi\phi}, \Gamma_{\chi\chi} \rightarrow 0.1\alpha^2 M \sim 10^{-5}M$ were kept in order to define the spectral function.

but no widths (“screened”), and the full system including the widths (“damped”). The results are illustrated in fig. 8. The screened Sommerfeld enhancement is observed to be active even below the second threshold. The shifts of both thresholds to the left of the “free” ones reflect the Salpeter correction discussed in eq. (2.1). The inclusion of damping smoothens the spectral functions. After integration over the energies according to eq. (3.16), thermal effects get however largely hidden, apart from an overall suppression by $\exp(-2\Delta M/T)$ of annihilations in the $\chi\chi$ -channel. In a complete phenomenological analysis it should also be noted that the χ particles decay into the ϕ ones after thermal freeze-out, cf. e.g. ref. [67].

If ΔM is increased so that $\Delta M \gg \alpha^2 M$, the numerical determination of ρ_ϕ becomes challenging,¹² and a description of the system through a potential model eventually breaks down.

¹²The numerics can be modestly accelerated by noting that the off-diagonal terms in eq. (7.17) become small for large distances. Therefore, for $\rho \gg 1$ the equation satisfied by the homogeneous solution reads $(\partial_\rho^2 + x + i\epsilon)u_0^\phi = 0$, and correspondingly for u_0^χ . This can be solved as $u_0^\phi = C \sin(\rho\sqrt{x+i\epsilon} + \delta)$, $C, \delta \in \mathbb{C}$. Given that $\sqrt{x+i\epsilon}/\sin^2(\rho\sqrt{x+i\epsilon} + \delta) = -\partial_\rho \cot(\rho\sqrt{x+i\epsilon} + \delta)$, the integral $\int_{\rho_0}^\infty d\rho / (u_0^\phi)^2$ can be carried out. Both ends contribute, with $\lim_{\rho \rightarrow \infty} \cot(\rho\sqrt{x+i\epsilon} + \delta) = -i$. Subsequently C and δ can be traded for $u_0^\phi(\rho_0)$ and $u_0^{\phi'}(\rho_0)$. For $\rho_0 \gg 1$, we thus obtain

$$\int_{\rho_0}^\infty d\rho \operatorname{Im} \left[\frac{1}{(u_0^\phi)^2} \right] = \operatorname{Im} \left\{ \frac{1}{u_0^\phi(\rho_0) [u_0^{\phi'}(\rho_0) - i\sqrt{x+i\epsilon} u_0^\phi(\rho_0)]} \right\}. \quad (7.19)$$

In the free limit this result can also be used at $\rho_0 \ll 1$ where, recalling the asymptotics $u_0^\phi(\rho_0) \approx \rho_0$, $u_0^{\phi'}(\rho_0) \approx 1$, it produces $\rho_\phi = \frac{\alpha M^2}{4\pi} \operatorname{Re} \sqrt{x+i\epsilon}$, in accordance with eq. (3.17).

Physically we expect the potential generated by the virtual exchange to become suppressed for $2\Delta M - E' \gg \alpha^2 M$, and correspondingly the Sommerfeld enhancement experienced by the ϕ -particles to only be re-instated somewhat below the heavier threshold, but it would be interesting to understand this quantitatively.

7.4. Summary of the non-degenerate situation

The purpose of this section has been to show that Sommerfeld enhancement does remain active when $\Delta M \sim \alpha^2 M > 0$. To be more precise, there are different cases of gauge exchange between non-degenerate particles. With the process in fig. 1(b), it is possible to have a kinematically permitted configuration with static on-shell DM and DM' particles and the energy flow $\pm\Delta M$ through the gauge line. Therefore the nature of gauge exchange gets modified only if $\Delta M \gtrsim m_{\text{th}} \sim \alpha^{1/2} T$. In contrast, the process in fig. 1(a) leads to a non-trivial quantum-mechanical behaviour. Naively, one could think that if we are below the threshold for the production of the heavier particles ($E_{\text{kin}} < 2\Delta M$), the lighter ones have no partners to interact with, and they should feel no Sommerfeld enhancement. This is not true: the heavier ones can appear as virtual states, and in fact they thereby generate an attractive interaction between the lighter ones. Therefore, at least if $\Delta M \lesssim \alpha^2 M$, the Sommerfeld effect is present even below the heavier threshold, just suppressed somewhat by Debye screening.

8. Effects from different colour and spin decompositions

If the gauge group is unbroken and non-Abelian, then the annihilating pair can appear in different (global) gauge representations. Within perturbation theory the representation dictates whether the gauge force between the two particles is attractive or repulsive. Presumably, the different representations appear with specific weights in the (perturbative) thermal ensemble. Thereby the total annihilation rate is a certain combination of the contributions of the different gauge representations (for a discussion cf. e.g. ref. [68]). The purpose of this section is to recall how the contributions of all gauge decompositions, and also of the various spin states, can be included with their proper thermal weights and in a gauge-independent manner in the total thermal annihilation rate.

Within the NRQCD framework, annihilations through various gauge and spin channels, as well as channels suppressed by higher powers of the relative velocity, correspond to unique local gauge-invariant four-particle operators [20]. The four-particle operators originate from integrating out the energy scale $2M \gg \pi T$; therefore, the determination of the coefficients can be carried out with vacuum perturbation theory.

Thermal effects originate when we compute the thermal expectations values of the operators, in the sense of eq. (3.2). Assuming now η and θ to be 2-component spinors, spin effects

originate from structures of the type $\eta^T \sigma_i \theta$, and gauge effects from the type $\eta^T T^a \theta$, where σ_i is a Pauli matrix and T^a is a generator of the gauge group. The sum over m in eq. (3.2) is taken over the full ensemble. A spectral function can be defined like in sec. 3.2, and the total rate from every particular operator reduced to its Laplace transform like in eq. (3.16).

The essential question is how the Schrödinger equation of sec. 3.3 depends on the channel in question. The source term in eq. (3.13), which is independent of the coupling, is modified in a trivial way, with N replaced by an appropriate factor. The dynamical information concerning the attractive or repulsive nature of the interaction is encoded in the potential V and the width Γ , to be computed in the appropriate representation.¹³

It may be asked whether the Schrödinger equations for the different channels couple to each other, similarly to eq. (7.17). In general, different gauge representations do *not* couple. In order to illustrate the argument in concrete terms, consider the QCD-like decomposition $\mathbf{3} \otimes \mathbf{3}^* = \mathbf{1} \oplus \mathbf{8}$. The symmetry in question is, however, a gauge symmetry: a singlet representation can convert into an octet only by simultaneously emitting a colour-electric dipole $\sim \mathbf{r} \cdot g\mathbf{E}^a$, or another excitation with the same quantum numbers. Since these are not among our effective low-energy variables, a mixing is forbidden. Indeed, within the PNRQCD framework, the width Γ appearing in the singlet channel can be shown to get a contribution precisely from the possibility that the singlet split into an octet and a colour-electric-dipole, after integrating out the latter two [43]. Therefore the octet states have already been accounted for within the singlet computation.

For the case of spin channels, we also expect orthogonality in general, given that gauge exchange is spin independent to leading order in $1/M$. At higher orders, the presence or not of a coupling can be checked through an analysis like in sec. 7.2, which also establishes whether the exchange in the given channel is attractive or repulsive.

To summarize, the first step is to determine all absorptive operators in the sense of ref. [20]. In a resummed perturbative approach, we subsequently compute the spectral functions for each of them, and then take the Laplace transform in eq. (3.16). The total annihilation rate is the sum of the contributions of the various operators, i.e. the channels are summed together at the level of total rates.

9. Conclusions

The purpose of this paper has been to revisit the s -wave thermal annihilation rate of massive neutral particles relevant for cosmology. The formalism is based on non-relativistic effective theories [19, 20] in combination with a Hard Thermal Loop [27, 45–47] resummed treatment of thermal contributions. The basic object addressed is a spectral function, i.e. the imaginary

¹³It should be noted that in non-singlet channels the spectral function is *not* manifestly gauge independent; nevertheless the total annihilation rate, which can also be measured non-perturbatively, is so [18].

part of a Green’s function, which can be interpreted as a differential annihilation rate. The total annihilation rate is obtained from a Laplace transform of the spectral function, cf. eq. (3.16). The dark matter particles are assumed to interact through a “mediator”, which for illustration is taken to be a gauge field, characterized by a fine-structure constant α .

The Laplace transform in eq. (3.16) shows that the spectral function is needed for $|\omega - 2M| \lesssim \pi T \ll M$, i.e. deep in the non-relativistic regime. Even though NLO computations of thermal corrections, and higher-order computations of vacuum corrections, have been carried out for spectral functions of this type, and even though they do yield formally well-behaved results, they show in general poor convergence. Moreover, a strict NLO computation suggests that thermal corrections are power-suppressed (cf. e.g. refs. [30, 31]), which is not the case in general (cf. the Salpeter correction in eq. (2.1)). To properly understand the system in the non-relativistic regime therefore requires a resummed treatment.

Resummations can be implemented through a numerical solution of an inhomogeneous Schrödinger equation (cf. eqs. (3.13) and (3.14)), with a static potential incorporating thermal corrections such as Debye screening and Landau damping. The latter originates from real scatterings of the mediators with plasma particles, as is illustrated in some detail around eqs. (A.11) and (A.12). Our hope is that theoretical uncertainties of freeze-out computations can be scrutinized and ultimately reduced through this approach.

In terms of power counting, thermal effects on the differential annihilation rate around the threshold ($|\omega - 2M| \lesssim \alpha^2 M$) are of order unity for $T \gtrsim \alpha M$ (cf. eq. (2.3)). In contrast, the total annihilation rate gets an $\gtrsim \mathcal{O}(1)$ contribution from the threshold region only for $T \lesssim \alpha^2 M$ (cf. eq. (2.2)). For weak interactions with $\alpha \sim 0.01$, the freeze-out regime $T \sim M/25 \dots M/20$ corresponds roughly speaking to $T \gtrsim \alpha M$. Therefore we expect a large thermal effect on the differential annihilation rate but only a higher-order correction to the total rate. For strong interactions with $\alpha = g^2 C_R / (4\pi) \gtrsim 0.1$, in contrast, the freeze-out regime may correspond to $T \sim \alpha^2 M$, and the threshold region could dominate the total rate.

In order to consolidate these parametric estimates, we have carried out numerical studies of semi-realistic models. For a purely weakly interacting case along the classic WIMP paradigm, our basic finding is that even if bound states were to exist at zero temperature, they are completely melted around the freeze-out temperature (cf. figs. 3, 4). The spectral function does get smoothened across the two-particle threshold by thermal effects. Nevertheless, for TeV range masses, the total annihilation rate, which gets a contribution from a broad energy range, is remarkably well (within $\sim 1\%$) predicted by a thermally averaged purely Coulombic Sommerfeld factor, and even better if Debye screening is accounted for.

Permitting for some non-degeneracy in the dark particle spectrum, we subsequently demonstrated that the details of the “coupled-channel” dynamics are delicate (cf. sec. 7). If the mass splitting is not too large, we however expect the Sommerfeld enhancement, modified by thermal screening, to remain active even below the heavier threshold (cf. fig. 8).

Apart from weakly interacting cases, there are models involving strongly interacting dark matter candidates, or strongly interacting particles interacting with the dark matter ones. In this paper we considered the case of gluinos, for which the importance of bound-state effects had already been recognized and treated through a phenomenological modification of Boltzmann equations [14, 61]. We confirm that bound states persist up to the temperatures relevant for the freeze-out process (cf. fig. 5), and can boost the annihilation rate by a factor $\sim 4\ldots 80$ compared with a Sommerfeld-enhanced computation which in itself boosts the annihilation rate by a similar factor compared with a naive estimate (cf. fig. 6). The numerically coincident magnitude of the two effects is in nice accordance with the parametric estimate around eq. (2.2), showing that both effects become large in the same temperature range. We stress that within our formalism the existence or melting of bound states does not need to be known in advance, but comes out from the analysis. Evaluating the phenomenological significance of these findings requires a complete model-specific study, which goes beyond the scope of this paper.

Acknowledgements

M.L. thanks S. Biondini and M. Garny for valuable discussions. S.K. was supported by the National Research Foundation of Korea under grant No. 2015R1A2A2A01005916 funded by the Korean government (MEST). M.L. was supported by the Swiss National Science Foundation (SNF) under grant 200020-168988, and by the Munich Institute for Astro- and Particle Physics (MIAPP) of the DFG cluster of excellence “Origin and Structure of the Universe”.

Appendix A. Neutral gauge field self-energies in the Standard Model

We present in this appendix the 1-loop thermal self-energy matrix of neutral gauge bosons in the Standard Model. Results are given in a general R_ξ gauge, and amount to simple generalizations of classic results for the vacuum case (cf. e.g. ref. [69] and references therein). Only terms contributing to the transverse part of the self-energy are shown. We introduce the notation

$$A(m) \equiv \oint_P \frac{1}{P^2 + m^2}, \quad (\text{A.1})$$

$$B(K; m_1, m_2) \equiv \oint_P \frac{1}{(P^2 + m_1^2)[(P + K)^2 + m_2^2]}, \quad (\text{A.2})$$

$$B_{\mu\nu}(K; m_1, m_2) \equiv \oint_P \frac{P_\mu P_\nu}{(P^2 + m_1^2)[(P + K)^2 + m_2^2]}, \quad (\text{A.3})$$

where $K = (k_n, \mathbf{k})$ is a Euclidean four-vector and the imaginary-time formalism is employed. The sum-integrals \mathfrak{F}_P and $\mathfrak{F}_{\{P\}}$ go over bosonic and fermionic Matsubara momenta, respectively; in the fermionic case the structures are denoted by \tilde{A} , \tilde{B} and $\tilde{B}_{\mu\nu}$. With this notation and letting $m'_W \equiv \xi^{1/2} m_W$, where ξ is a gauge parameter, the hypercharge part of the (bare) transverse self-energy matrix reads

$$\begin{aligned}
\Pi_{11;\mu\nu} = & g_1^2 \left\{ -B_{\mu\nu}(K; m_h, m_Z) - \delta_{\mu\nu} m_Z^2 B(K; m_h, m_Z) - \frac{\delta_{\mu\nu} A(m_h)}{2} \right. \\
& - 2B_{\mu\nu}(K; m_W, m'_W) - 2\delta_{\mu\nu} m_W^2 B(K; m_W, m'_W) + B_{\mu\nu}(K; m'_W, m'_W) \\
& + \frac{17}{3} \left[\tilde{B}_{\mu\nu}(K; m_t, m_t) - \frac{\delta_{\mu\nu} \tilde{A}(m_t)}{2} + \delta_{\mu\nu} \left(\frac{K^2}{4} + \frac{9m_t^2}{34} \right) \tilde{B}(K; m_t, m_t) \right] \\
& + \frac{40n_G - 17}{3} \left[\tilde{B}_{\mu\nu}(K; 0, 0) - \frac{\delta_{\mu\nu} \tilde{A}(0)}{2} + \frac{\delta_{\mu\nu} K^2 \tilde{B}(K; 0, 0)}{4} \right] \\
& \left. - \frac{(D-1)\delta_{\mu\nu}}{2m_h^2} \left[2m_W^2 A(m_W) + m_Z^2 A(m_Z) \right] + \frac{6\delta_{\mu\nu} m_t^2 \tilde{A}(m_t)}{m_h^2} \right\}. \tag{A.4}
\end{aligned}$$

Here m_h and m_t are the Higgs and top masses, $n_G = 3$ is the number of generations, and $D = 4 - 2\epsilon$ is the dimensionality of space-time. The mixed part takes the form

$$\begin{aligned}
\Pi_{12;\mu\nu} = & g_1 g_2 \left\{ -B_{\mu\nu}(K; m_h, m_Z) - \delta_{\mu\nu} m_Z^2 B(K; m_h, m_Z) - \frac{\delta_{\mu\nu} A(m_h)}{2} \right. \\
& + B_{\mu\nu}(K; m'_W, m'_W) - \delta_{\mu\nu} A(m'_W) \\
& - \tilde{B}_{\mu\nu}(K; m_t, m_t) + \frac{\delta_{\mu\nu} \tilde{A}(m_t)}{2} + \delta_{\mu\nu} \left(-\frac{K^2}{4} + \frac{3m_t^2}{2} \right) \tilde{B}(K; m_t, m_t) \\
& + \tilde{B}_{\mu\nu}(K; 0, 0) - \frac{\delta_{\mu\nu} \tilde{A}(0)}{2} + \frac{\delta_{\mu\nu} K^2 \tilde{B}(K; 0, 0)}{4} \\
& \left. - \frac{(D-1)\delta_{\mu\nu}}{2m_h^2} \left[2m_W^2 A(m_W) + m_Z^2 A(m_Z) \right] + \frac{6\delta_{\mu\nu} m_t^2 \tilde{A}(m_t)}{m_h^2} \right\}. \tag{A.5}
\end{aligned}$$

Finally, the SU(2) part can be expressed as

$$\begin{aligned}
\Pi_{22;\mu\nu} = & g_2^2 \left\{ -B_{\mu\nu}(K; m_h, m_Z) - \delta_{\mu\nu} m_Z^2 B(K; m_h, m_Z) - \frac{\delta_{\mu\nu} A(m_h)}{2} \right. \\
& + \left(1 - \frac{K^4}{m_W^4} \right) B_{\mu\nu}(K; m'_W, m'_W) + 2 \left(1 + \frac{K^2}{m_W^2} \right)^2 B_{\mu\nu}(K; m_W, m'_W) \\
& + 2\delta_{\mu\nu} \frac{(K^2 + m_W^2)^2}{m_W^2} [B(K; m_W, m'_W) - B(K; m_W, m_W)] \\
& - 4 \left(D - 1 + \frac{K^2}{m_W^2} + \frac{K^4}{4m_W^4} \right) B_{\mu\nu}(K; m_W, m_W) + 2\delta_{\mu\nu} (m_W^2 - 2K^2) B(K; m_W, m_W) \\
& \left. + 2\delta_{\mu\nu} \left(D - 1 + \frac{K^2}{m_W^2} \right) A(m_W) - 2\delta_{\mu\nu} \left(1 + \frac{K^2}{m_W^2} \right) A(m'_W) \right\}
\end{aligned}$$

$$\begin{aligned}
& + 3 \left[\tilde{B}_{\mu\nu}(K; m_t, m_t) - \frac{\delta_{\mu\nu} \tilde{A}(m_t)}{2} + \delta_{\mu\nu} \left(\frac{K^2}{4} + \frac{m_t^2}{2} \right) \tilde{B}(K; m_t, m_t) \right] \\
& + (8n_G - 3) \left[\tilde{B}_{\mu\nu}(K; 0, 0) - \frac{\delta_{\mu\nu} \tilde{A}(0)}{2} + \frac{\delta_{\mu\nu} K^2 \tilde{B}(K; 0, 0)}{4} \right] \\
& - \frac{(D-1) \delta_{\mu\nu}}{2m_h^2} \left[2m_W^2 A(m_W) + m_Z^2 A(m_Z) \right] + \frac{6\delta_{\mu\nu} m_t^2 \tilde{A}(m_t)}{m_h^2} \Big\} . \tag{A.6}
\end{aligned}$$

The self-energies in eqs. (A.4)–(A.6) are gauge dependent. Gauge-independent expressions are obtained for two linear combinations, $\Pi_Z \equiv \sin^2(\theta) \Pi_{11} + \sin(2\theta) \Pi_{12} + \cos^2(\theta) \Pi_{22}$ evaluated at the Z pole $K = -im_Z$, and $\Pi_\gamma \equiv \cos^2(\theta) \Pi_{11} - \sin(2\theta) \Pi_{12} + \sin^2(\theta) \Pi_{22}$ evaluate at the γ pole $K = 0$. However at $\pi T \gg m_Z$ the vacuum poles are no longer relevant. Indeed there is a third limit, the so-called Hard Thermal Loop (HTL) one [27, 45–47], in which eqs. (A.4)–(A.6) are separately gauge-independent, as we now show.

As a first step, let us write down the thermal parts of the “master” sum-integrals in eqs. (A.1)–(A.3). For this purpose we keep $k \equiv |\mathbf{k}| \neq 0$ and work out the expressions up to and including $\mathcal{O}(\omega)$ after the analytic continuation $k_n \rightarrow -i[\omega + i0^+]$. Denoting $\int_{\mathbf{p}} = \frac{1}{2} \int_{-1}^{+1} dz \int_p$, where z is an angular variable, and omitting the vacuum parts, we get

$$A^{(T)}(m) = \int_p \frac{n_B(\epsilon)}{\epsilon} , \tag{A.7}$$

$$\begin{aligned}
B^{(T)}(-i[\omega + i0^+], \mathbf{k}; m_1, m_2) &= \int_p \left\{ \frac{n_B(\epsilon_1)}{4pk\epsilon_1} \ln \left| \frac{m_2^2 - m_1^2 + k^2 + 2pk}{m_2^2 - m_1^2 + k^2 - 2pk} \right| + \frac{n_B(\epsilon_2)}{4pk\epsilon_2} \ln \left| \frac{m_1^2 - m_2^2 + k^2 + 2pk}{m_1^2 - m_2^2 + k^2 - 2pk} \right| \right\} \\
&+ \frac{i\omega}{8\pi kT} \int_{\epsilon_{\min}}^{\infty} d\epsilon n_B(\epsilon) [1 + n_B(\epsilon)] + \mathcal{O}(\omega^2) , \tag{A.8}
\end{aligned}$$

$$\begin{aligned}
B_{00}^{(T)}(-i[\omega + i0^+], \mathbf{k}; m_1, m_2) &= - \int_p \left\{ \frac{\epsilon_1 n_B(\epsilon_1)}{4pk} \ln \left| \frac{m_2^2 - m_1^2 + k^2 + 2pk}{m_2^2 - m_1^2 + k^2 - 2pk} \right| + \frac{\epsilon_2 n_B(\epsilon_2)}{4pk} \ln \left| \frac{m_1^2 - m_2^2 + k^2 + 2pk}{m_1^2 - m_2^2 + k^2 - 2pk} \right| \right\} \\
&- \frac{i\omega}{8\pi kT} \int_{\epsilon_{\min}}^{\infty} d\epsilon \epsilon^2 n_B(\epsilon) [1 + n_B(\epsilon)] + \mathcal{O}(\omega^2) , \tag{A.9}
\end{aligned}$$

where

$$\epsilon_i \equiv \sqrt{p^2 + m_i^2} , \quad \epsilon_{\min} \equiv \frac{\sqrt{k^4 + 2k^2(m_1^2 + m_2^2) + (m_1^2 - m_2^2)^2}}{2k} . \tag{A.10}$$

The fermionic cases are obtained by replacing $n_B \rightarrow -n_F$.

Given that the imaginary parts play an important role in the analysis, let us detail their physical origin. Consider a space-like vector boson, with energy ω and momentum $k > \omega$, scattering on energetic plasma particles. For illustration, assume the plasma particles to be bosons and consider the case that they do not change their identity in the scattering, i.e. $m_1 = m_2$. Incorporating both reactions and inverse reactions, i.e. a decay and generation of

a vector boson with 4-momentum (ω, \mathbf{k}) , the scattering rate for a process in which the matrix element is proportional to the energy of a scatterer takes the form

$$\begin{aligned}
& \begin{array}{c} (\epsilon_p, \mathbf{p}) \\ \diagup \\ (\omega, \mathbf{k}) \text{ wavy line} \\ \diagdown \\ (\epsilon_{p+k}, \mathbf{p}+\mathbf{k}) \end{array} - \begin{array}{c} (\epsilon_p, \mathbf{p}) \\ \diagdown \\ (\omega, \mathbf{k}) \text{ wavy line} \\ \diagup \\ (\epsilon_{p+k}, \mathbf{p}+\mathbf{k}) \end{array} \quad (\text{A.11}) \\
&= \int_{\mathbf{p}} \frac{\epsilon_p^2}{4\epsilon_p \epsilon_{p+k}} \left\{ n_B(\epsilon_p) [1 + n_B(\epsilon_{p+k})] - n_B(\epsilon_{p+k}) [1 + n_B(\epsilon_p)] \right\} 2\pi \delta(\omega + \epsilon_p - \epsilon_{p+k}) \\
&= \int_{\mathbf{p}} \frac{\epsilon_p^2}{4\epsilon_p \epsilon_{p+k}} \left\{ n_B(\epsilon_p) - n_B(\epsilon_p + \omega) \right\} 2\pi \delta(\omega + \epsilon_p - \epsilon_{p+k}) \\
&= -\omega \pi \int_{\mathbf{p}} \frac{\epsilon_p}{2\epsilon_{p+k}} n'_B(\epsilon_p) \delta(\epsilon_p - \epsilon_{p+k}) + \mathcal{O}(\omega^2) \\
&= -\omega \pi \int_{\mathbf{p}} \epsilon_p n'_B(\epsilon_p) \delta(\epsilon_p^2 - \epsilon_{p+k}^2) + \mathcal{O}(\omega^2) \\
&= -\frac{\omega \pi}{2} \int_p \epsilon_p n'_B(\epsilon_p) \int_{-1}^{+1} dz \delta(k^2 + 2pkz) + \mathcal{O}(\omega^2) \\
&= \frac{\omega \pi}{4kT} \int_p \frac{\epsilon_p n_B(\epsilon_p) [1 + n_B(\epsilon_p)] \theta(2p - k)}{p} + \mathcal{O}(\omega^2) \\
&= \frac{\omega}{8\pi kT} \int_{\epsilon_{\min}}^{\infty} d\epsilon \epsilon^2 n_B(\epsilon) [1 + n_B(\epsilon)] + \mathcal{O}(\omega^2). \quad (\text{A.12})
\end{aligned}$$

This is a special case of the last line of eq. (A.9), and indicates that the imaginary part originates from real scatterings experienced by space-like gauge fields.

We now turn to the HTL limit [27, 45–47]. It corresponds to the approximation $\pi T \gg m, k$, and concerns terms which scale as T^2 . The sum-integral $B^{(T)}$ is of $\mathcal{O}(\ln(T/m))$ and therefore gives no HTL structure. The non-vanishing HTL structures read, for $D = 4$,

$$A^{(T)} \rightarrow \frac{T^2}{12}, \quad (\text{A.13})$$

$$B_{00}^{(T)} \rightarrow -\frac{T^2}{24} \left[1 + \frac{i\omega\pi}{k} + \mathcal{O}(\omega^2) \right], \quad (\text{A.14})$$

$$\tilde{A}^{(T)} \rightarrow -\frac{T^2}{24}, \quad (\text{A.15})$$

$$\tilde{B}_{00}^{(T)} \rightarrow \frac{T^2}{48} \left[1 + \frac{i\omega\pi}{k} + \mathcal{O}(\omega^2) \right]. \quad (\text{A.16})$$

After inserting these, eqs. (A.4)–(A.6) reduce to gauge-independent expressions:

$$\Pi_{11;00}^{(T)} \rightarrow -\frac{g_1^2 T^2}{8} \left(1 + \frac{2m_W^2 + m_Z^2 + 2m_t^2}{m_h^2} \right) + m_{E1}^2 \left(1 + \frac{i\omega\pi}{2k} \right) + \mathcal{O}(\omega^2), \quad (\text{A.17})$$

$$\Pi_{12;00}^{(T)} \rightarrow -\frac{g_1 g_2 T^2}{8} \left(1 + \frac{2m_W^2 + m_Z^2 + 2m_t^2}{m_h^2} \right) + \mathcal{O}(\omega^2), \quad (\text{A.18})$$

$$\Pi_{22;00}^{(T)} \rightarrow -\frac{g_2^2 T^2}{8} \left(1 + \frac{2m_W^2 + m_Z^2 + 2m_t^2}{m_h^2} \right) + m_{E2}^2 \left(1 + \frac{i\omega\pi}{2k} \right) + \mathcal{O}(\omega^2), \quad (\text{A.19})$$

where m_{E1}^2 and m_{E2}^2 are from eq. (4.4). Combined with tree-level effects from the Higgs mechanism, *viz.* $\Pi_{ij;00}^{(0)} = g_i g_j v_0^2/4$, the first parts of eqs. (A.17)–(A.19) can be accounted for through a T -dependent Higgs expectation value, $\Pi_{ij;00}^{(0)} + \Pi_{ij;00}^{(T)} = g_i g_j v_T^2/4 + \dots$, where

$$v_T^2 \equiv -\frac{m_\phi^2}{\lambda} \text{ for } m_\phi^2 < 0, \quad m_\phi^2 \equiv -\frac{m_h^2}{2} + \frac{(g_1^2 + 3g_2^2 + 8\lambda + 4h_t^2)T^2}{16}. \quad (\text{A.20})$$

Subsequently we redefine m_W and m_Z to stand for the gauge boson masses defined with v_T .

The propagators corresponding to the HTL self-energies in eqs. (A.17)–(A.19) can be obtained through straightforward inversion. Since only the small- ω limit is needed, the terms proportional to ω can be expanded to first order. Projecting the matrix subsequently to the Z direction, the retarded Z propagator becomes

$$\langle Z_0 Z_0 \rangle_{\text{R}} = (\sin \theta \ \cos \theta) \left(\Delta - \Delta \Omega \Delta \right) \begin{pmatrix} \sin \theta \\ \cos \theta \end{pmatrix} + \mathcal{O}(\omega^2), \quad (\text{A.21})$$

where Δ can be diagonalized through a rotation by the angle $\tilde{\theta}$ defined in eq. (4.3),

$$\Delta = \begin{pmatrix} \cos \tilde{\theta} & \sin \tilde{\theta} \\ -\sin \tilde{\theta} & \cos \tilde{\theta} \end{pmatrix} \begin{pmatrix} \frac{1}{k^2 + m_{\tilde{Q}}^2} & 0 \\ 0 & \frac{1}{k^2 + m_Z^2} \end{pmatrix} \begin{pmatrix} \cos \tilde{\theta} & -\sin \tilde{\theta} \\ \sin \tilde{\theta} & \cos \tilde{\theta} \end{pmatrix}. \quad (\text{A.22})$$

The masses are given in eq. (4.5). The width matrix reads

$$\Omega = \frac{i\omega\pi}{2k} \begin{pmatrix} m_{E1}^2 & 0 \\ 0 & m_{E2}^2 \end{pmatrix}. \quad (\text{A.23})$$

Consequently the static limit of the time-ordered propagator, eq. (3.23), becomes

$$\begin{aligned} \lim_{\omega \rightarrow 0} i \langle Z_0 Z_0 \rangle_{\text{T}}(\omega, k) &= \frac{\cos^2(\tilde{\theta} - \theta)}{k^2 + m_Z^2} + \frac{\sin^2(\tilde{\theta} - \theta)}{k^2 + m_{\tilde{Q}}^2} \\ &- \frac{i\pi T}{k} \left\{ m_{E1}^2 \left[\frac{\sin \tilde{\theta} \cos(\tilde{\theta} - \theta)}{k^2 + m_Z^2} - \frac{\cos \tilde{\theta} \sin(\tilde{\theta} - \theta)}{k^2 + m_{\tilde{Q}}^2} \right]^2 \right. \\ &\quad \left. + m_{E2}^2 \left[\frac{\cos \tilde{\theta} \cos(\tilde{\theta} - \theta)}{k^2 + m_Z^2} + \frac{\sin \tilde{\theta} \sin(\tilde{\theta} - \theta)}{k^2 + m_{\tilde{Q}}^2} \right]^2 \right\}. \quad (\text{A.24}) \end{aligned}$$

The two terms in the imaginary part correspond to real scatterings through hypercharge and weak interactions, respectively. Eq. (A.24) leads directly to eqs. (4.7) and (4.8).

Finally, for completeness, we also give the time-ordered W propagator:

$$\lim_{\omega \rightarrow 0} i \langle W_0^a W_0^{a'} \rangle_{\text{T}}(\omega, k) = \delta^{aa'} \left\{ \frac{1}{k^2 + m_W^2} - \frac{i\pi T}{k} \frac{m_{E2}^2}{(k^2 + m_W^2)^2} \right\}. \quad (\text{A.25})$$

Here $a, a' \in \{1, 2\}$ and $m_W^2 \equiv m_W^2 + m_{E2}^2$, where m_{E2}^2 is from eq. (4.4).

Appendix B. Gauge field self-energy in a dark U(1) model

In this appendix we present the 1-loop thermal self-energy matrix of Z' gauge bosons (mass m_V) interacting with a dark scalar field (mass m_S), which breaks the gauge symmetry. Only the transverse part of the self-energy is shown. Making use of the notation in eqs. (A.1)–(A.3) it reads

$$\begin{aligned} \Pi_{\mu\nu} = & -2e'^2 \left\{ 2B_{\mu\nu}(K; m_S, m_V) + 2\delta_{\mu\nu} m_V^2 B(K; m_S, m_V) \right. \\ & \left. + \delta_{\mu\nu} A(m_S) + \frac{(D-1)\delta_{\mu\nu} m_V^2 A(m_V)}{m_S^2} \right\}. \end{aligned} \quad (\text{B.1})$$

Carrying out analytic continuation, $k_n \rightarrow -i(\omega + i0^+)$, and taking the HTL limit, cf. eqs. (A.13)–(A.16), we get

$$\Pi_{00}^{(T)} \rightarrow e'^2 \left\{ -\frac{T^2}{3} \left(1 + \frac{3m_V^2}{2m_S^2} \right) + \frac{T^2}{3} \left(1 + \frac{i\omega\pi}{2k} \right) + \mathcal{O}(\omega^2) \right\}. \quad (\text{B.2})$$

Combined with the tree-level effect from the Higgs mechanism, *viz.* $\Pi_{00}^{(0)} = e'^2 v_0'^2$, the first part of eq. (B.2) can be accounted for through a temperature dependent Higgs expectation value, $\Pi_{00}^{(0)} + \Pi_{00}^{(T)} = e'^2 v_T'^2 + \dots$, where

$$v_T'^2 \equiv -\frac{m_{\phi'}^2}{\lambda'} \text{ for } m_{\phi'}^2 < 0, \quad m_{\phi'}^2 \equiv -\frac{m_S^2}{2} + \frac{(3e'^2 + 4\lambda')T^2}{12}. \quad (\text{B.3})$$

Subsequently we redefine m_V as $m_V \equiv e'v_T'$. The latter term in eq. (B.2) is parametrized by the Debye mass m_{E}^2 defined in eq. (5.2).

The resummed time-ordered propagator can now be computed from eq. (3.23), yielding

$$\lim_{\omega \rightarrow 0} i\langle V_0 V_0 \rangle_{\text{T}}(\omega, k) = \frac{1}{k^2 + m_V^2 + m_{\text{E}}^2} - \frac{i\pi T}{k} \frac{m_{\text{E}}^2}{(k^2 + m_V^2 + m_{\text{E}}^2)^2}. \quad (\text{B.4})$$

This directly leads to eq. (5.3).

References

- [1] K. Griest and D. Seckel, *Three exceptions in the calculation of relic abundances*, Phys. Rev. D 43 (1991) 3191.
- [2] P. Gondolo and G. Gelmini, *Cosmic abundances of stable particles: Improved analysis*, Nucl. Phys. B 360 (1991) 145.
- [3] J. Hisano, S. Matsumoto, M. Nagai, O. Saito and M. Senami, *Non-perturbative effect on thermal relic abundance of dark matter*, Phys. Lett. B 646 (2007) 34 [hep-ph/0610249].

- [4] M. Cirelli, A. Strumia and M. Tamburini, *Cosmology and Astrophysics of Minimal Dark Matter*, Nucl. Phys. B 787 (2007) 152 [0706.4071].
- [5] J.L. Feng, M. Kaplinghat and H.-B. Yu, *Sommerfeld Enhancements for Thermal Relic Dark Matter*, Phys. Rev. D 82 (2010) 083525 [1005.4678].
- [6] M. Pospelov and A. Ritz, *Astrophysical Signatures of Secluded Dark Matter*, Phys. Lett. B 671 (2009) 391 [0810.1502].
- [7] M. Ibe, H. Murayama and T.T. Yanagida, *Breit-Wigner Enhancement of Dark Matter Annihilation*, Phys. Rev. D 79 (2009) 095009 [0812.0072].
- [8] J.D. March-Russell and S.M. West, *WIMPonium and Boost Factors for Indirect Dark Matter Detection*, Phys. Lett. B 676 (2009) 133 [0812.0559].
- [9] W. Shepherd, T.M.P. Tait and G. Zaharijas, *Bound states of weakly interacting dark matter*, Phys. Rev. D 79 (2009) 055022 [0901.2125].
- [10] J.L. Feng, M. Kaplinghat, H. Tu and H.B. Yu, *Hidden Charged Dark Matter*, JCAP 07 (2009) 004 [0905.3039].
- [11] W. Detmold, M. McCullough and A. Pochinsky, *Dark Nuclei I: Cosmology and Indirect Detection*, Phys. Rev. D 90 (2014) 115013 [1406.2276].
- [12] M.B. Wise and Y. Zhang, *Stable Bound States of Asymmetric Dark Matter*, Phys. Rev. D 90 (2014) 055030; *ibid.* 91 (2015) 039907 (E) [1407.4121].
- [13] B. von Harling and K. Petraki, *Bound-state formation for thermal relic dark matter and unitarity*, JCAP 12 (2014) 033 [1407.7874].
- [14] J. Ellis, F. Luo and K.A. Olive, *Gluino Coannihilation Revisited*, JHEP 09 (2015) 127 [1503.07142].
- [15] K. Petraki, M. Postma and M. Wiechers, *Dark-matter bound states from Feynman diagrams*, JHEP 06 (2015) 128 [1505.00109].
- [16] K. Petraki, M. Postma and J. de Vries, *Radiative bound-state-formation cross-sections for dark matter interacting via a Yukawa potential*, 1611.01394.
- [17] T. Matsui and H. Satz, *J/ψ Suppression by Quark-Gluon Plasma Formation*, Phys. Lett. B 178 (1986) 416.
- [18] S. Kim and M. Laine, *Rapid thermal co-annihilation through bound states in QCD*, JHEP 07 (2016) 143 [1602.08105].

- [19] W.E. Caswell and G.P. Lepage, *Effective Lagrangians for Bound State Problems in QED, QCD, and Other Field Theories*, Phys. Lett. B 167 (1986) 437.
- [20] G.T. Bodwin, E. Braaten and G.P. Lepage, *Rigorous QCD analysis of inclusive annihilation and production of heavy quarkonium*, Phys. Rev. D 51 (1995) 1125; *ibid.* 55 (1997) 5853 (E) [hep-ph/9407339].
- [21] D. Bödeker and M. Laine, *Sommerfeld effect in heavy quark chemical equilibration*, JHEP 01 (2013) 037 [1210.6153].
- [22] A. Sommerfeld, *Über die Beugung und Bremsung der Elektronen*, Ann. Phys. (Leipzig) 403 (1931) 257.
- [23] L.D. Landau and E.M. Lifshitz, *Quantum Mechanics, Non-Relativistic Theory*, Third Edition, §136 (Butterworth-Heinemann, Oxford).
- [24] V. Fadin, V. Khoze and T. Sjöstrand, *On the threshold behavior of heavy top production*, Z. Phys. C 48 (1990) 613.
- [25] K. Blum, R. Sato and T.R. Slatyer, *Self-consistent Calculation of the Sommerfeld Enhancement*, JCAP 06 (2016) 021 [1603.01383].
- [26] L.S. Brown and R.F. Sawyer, *Nuclear reaction rates in a plasma*, Rev. Mod. Phys. 69 (1997) 411 [astro-ph/9610256].
- [27] R.D. Pisarski, *Scattering Amplitudes in Hot Gauge Theories*, Phys. Rev. Lett. 63 (1989) 1129.
- [28] G.D. Moore and D. Teaney, *How much do heavy quarks thermalize in a heavy ion collision?*, Phys. Rev. C 71 (2005) 064904 [hep-ph/0412346].
- [29] M. Laine, O. Philipsen, P. Romatschke and M. Tassler, *Real-time static potential in hot QCD*, JHEP 03 (2007) 054 [hep-ph/0611300].
- [30] J.F. Donoghue, B.R. Holstein and R.W. Robinett, *Quantum Electrodynamics at Finite Temperature*, Annals Phys. 164 (1985) 233; *ibid.* 172 (1986) 483 (E).
- [31] T. Wizansky, *Finite temperature corrections to relic density calculations*, Phys. Rev. D 74 (2006) 065007 [hep-ph/0605179].
- [32] P.M. Chesler, A. Gynther and A. Vuorinen, *On the dispersion of fundamental particles in QCD and $\mathcal{N} = 4$ Super Yang-Mills theory*, JHEP 09 (2009) 003 [0906.3052].
- [33] M.A. Escobedo and J. Soto, *Non-relativistic bound states at finite temperature (I): The Hydrogen atom*, Phys. Rev. A 78 (2008) 032520 [0804.0691].

- [34] M. Laine, *How to compute the thermal quarkonium spectral function from first principles?*, Nucl. Phys. A 820 (2009) 25C [0810.1112].
- [35] F. Dominguez and B. Wu, *On dissociation of heavy mesons in a hot quark-gluon plasma*, Nucl. Phys. A 818 (2009) 246 [0811.1058].
- [36] D. Bödeker and M. Laine, *Heavy quark chemical equilibration rate as a transport coefficient*, JHEP 07 (2012) 130 [1205.4987].
- [37] B.W. Lee and S. Weinberg, *Cosmological Lower Bound on Heavy Neutrino Masses*, Phys. Rev. Lett. 39 (1977) 165.
- [38] J. Bernstein, L.S. Brown and G. Feinberg, *The Cosmological Heavy Neutrino Problem Revisited*, Phys. Rev. D 32 (1985) 3261.
- [39] Y. Burnier, M. Laine and M. Vepsäläinen, *Heavy quark medium polarization at next-to-leading order*, JHEP 02 (2009) 008 [0812.2105].
- [40] M. Beneke, F. Dighera and A. Hryczuk, *Relic density computations at NLO: infrared finiteness and thermal correction*, JHEP 10 (2014) 45; *ibid.* 07 (2016) 106 (E) [1409.3049].
- [41] M. Laine, *A Resummed perturbative estimate for the quarkonium spectral function in hot QCD*, JHEP 05 (2007) 028 [0704.1720].
- [42] Y. Burnier, M. Laine and M. Vepsäläinen, *Heavy quarkonium in any channel in resummed hot QCD*, JHEP 01 (2008) 043 [0711.1743].
- [43] N. Brambilla, J. Ghiglieri, A. Vairo and P. Petreczky, *Static quark-antiquark pairs at finite temperature*, Phys. Rev. D 78 (2008) 014017 [0804.0993].
- [44] M.J. Strassler and M.E. Peskin, *Threshold production of heavy top quarks: QCD and the Higgs boson*, Phys. Rev. D 43 (1991) 1500.
- [45] J. Frenkel and J.C. Taylor, *High Temperature Limit of Thermal QCD*, Nucl. Phys. B 334 (1990) 199.
- [46] E. Braaten and R.D. Pisarski, *Soft Amplitudes in Hot Gauge Theories: a General Analysis*, Nucl. Phys. B 337 (1990) 569.
- [47] J.C. Taylor and S.M.H. Wong, *The Effective Action of Hard Thermal Loops in QCD*, Nucl. Phys. B 346 (1990) 115.
- [48] A. Beraudo, J.-P. Blaizot and C. Ratti, *Real and imaginary-time $Q\bar{Q}$ correlators in a thermal medium*, Nucl. Phys. A 806 (2008) 312 [0712.4394].

- [49] M. Le Bellac, *Thermal Field Theory* (Cambridge University Press, Cambridge, 2000).
- [50] M. Laine and A. Vuorinen, *Basics of Thermal Field Theory – A Tutorial on Perturbative Computations*, Lect. Notes Phys. 925 (2016) 1–281 [1701.01554].
- [51] Y. Akamatsu, *Heavy quark master equations in the Lindblad form at high temperatures*, Phys. Rev. D 91 (2015) 056002 [1403.5783].
- [52] S. Caron-Huot, *Hard thermal loops in the real-time formalism*, JHEP 04 (2009) 004 [0710.5726].
- [53] J. Ghiglieri and M. Laine, *Neutrino dynamics below the electroweak crossover*, JCAP 07 (2015) 015 [1605.07720].
- [54] M.E. Carrington, *The Effective potential at finite temperature in the Standard Model*, Phys. Rev. D 45 (1992) 2933.
- [55] M. Beneke *et al*, *Relic density of wino-like dark matter in the MSSM*, JHEP 03 (2016) 119 [1601.04718].
- [56] B. Holdom, *Two $U(1)$'s and ϵ Charge Shifts*, Phys. Lett. B 166 (1986) 196.
- [57] K.S. Babu, C.F. Kolda and J. March-Russell, *Implications of generalized $Z - Z'$ mixing*, Phys. Rev. D 57 (1998) 6788 [hep-ph/9710441].
- [58] M. Pospelov, A. Ritz and M.B. Voloshin, *Secluded WIMP Dark Matter*, Phys. Lett. B 662 (2008) 53 [0711.4866].
- [59] M. Cirelli, M. Kadastik, M. Raidal and A. Strumia, *Model-independent implications of the e^\pm , \bar{p} cosmic ray spectra on properties of Dark Matter*, Nucl. Phys. B 813 (2009) 1 [0809.2409].
- [60] N. Arkani-Hamed, D.P. Finkbeiner, T.R. Slatyer and N. Weiner, *A Theory of Dark Matter*, Phys. Rev. D 79 (2009) 015014 [0810.0713].
- [61] J. Ellis, J.L. Evans, F. Luo and K.A. Olive, *Scenarios for Gluino Coannihilation*, JHEP 02 (2016) 071 [1510.03498].
- [62] J. Ellis, K.A. Olive and J. Zheng, *The Extent of the Stop Coannihilation Strip*, Eur. Phys. J. C 74 (2014) 2947 [1404.5571].
- [63] J. Harz, B. Herrmann, M. Klasen, K. Kovařík and M. Meinecke, *SUSY-QCD corrections to stop annihilation into electroweak final states including Coulomb enhancement effects*, Phys. Rev. D 91 (2015) 034012 [1410.8063].

- [64] A. Ibarra, A. Pierce, N.R. Shah and S. Vogl, *Anatomy of Coannihilation with a Scalar Top Partner*, Phys. Rev. D 91 (2015) 095018 [1501.03164].
- [65] L. Lopez Honorez and C.E. Yaguna, *A new viable region of the inert doublet model*, JCAP 01 (2011) 002 [1011.1411].
- [66] C. Garcia-Cely, M. Gustafsson and A. Ibarra, *Probing the Inert Doublet Dark Matter Model with Cherenkov Telescopes*, JCAP 02 (2016) 043 [1512.02801].
- [67] F.S. Queiroz and C.E. Yaguna, *The CTA aims at the Inert Doublet Model*, JCAP 02 (2016) 038 [1511.05967].
- [68] A. De Simone, G.F. Giudice and A. Strumia, *Benchmarks for Dark Matter Searches at the LHC*, JHEP 06 (2014) 081 [1402.6287].
- [69] W.F.L. Hollik, *Radiative Corrections in the Standard Model and their Role for Precision Tests of the Electroweak Theory*, Fortsch. Phys. 38 (1990) 165.